947

THEORIE DE LA DIFFUSION

DANS LE PLAN

Thèse présentée à la Faculté des Sciences
de l'Université de Neuchâtel
pour obtenir le grade de docteur ès sciences
par

François Guillod

Ces trois articles représentent l'essentiel de ce travail de thèse.

IMPRIMATUR POUR LA THÈSE

Théorie de la diffusion dans le plan

de M*onsieur François Guillod*

UNIVERSITÉ DE NEUCHATEL

FACULTÉ DES SCIENCES

La Faculté des sciences de l'Université de Neuchâtel,
sur le rapport des membres du jury,

Messieurs P. Huguenin, J.-P. Amiet et

C. Wilkin (Londres)

autorise l'impression de la présente thèse.

Neuchâtel, le *12 juillet 1984*

Le doyen:

H. Beck

F. Guillod, P. Huguenin,
J. Phys. A15, 3705 (1982)

F. Guillod, P. Huguenin,
Phys. Lett. A101, 1 (1984)

F. Guillod, P. Huguenin,
Helv. Phys. Acta 57, 86 (1984)

Le texte complet de cette thèse est déposé chez Monsieur le Professeur P. Huguenin à l'Institut de Physique de l'Université de Neuchâtel.

Helvetica Physica Acta, Vol. 57 (1984) 86–95

0018-0238/84/010086-10$1.50 + 0.20/0

Geometrical approach to the Aharonov–Bohm plus potential scattering

By F. Guillod and P. Huguenin, Institut de Physique, 1 Rue A. Breguet, Université de Neuchâtel, CH-2000 Neuchâtel, Switzerland

(5. VII. 1983; rev. 30. IX. 1983)

Abstract. The ambiguity group of the canonical transformation which introduces the scattering variables 'deflection angle' and 'time delay' is not trivial. The restriction of the scattering operator to the invariant subspaces of the representations of this group leads exactly to the Aharonov–Bohm effect. Distinct values of the magnetic flux correspond to inequivalent representations.

1. Introduction

If you are interested in a non-linear canonical transformation $(q, p) \mapsto (\bar{q}, \bar{p})$ it will not be generally one-to-one. If this transformation has to be quantised, the operators associated to $(\bar{q}, \bar{p})$ will not have the same spectra than those associated to (q, p). Therefore, it is impossible to find a quantum unitary operator which corresponds to the classical canonical transformation.

In certain cases however, a group may be associated to a non-one-to-one canonical transformation. This group, called ambiguity group, has been introduced by Moshinsky and Seligman [1, 2, 3]. Owing to its representations an unitary operator can be constructed which corresponds to the canonical transformation.

In a previous paper, the notion of ambiguity group was applied to the scattering theory and it was suggested there that this formalism could explain geometrically the Aharonov–Bohm effect [4]. This point of view is now presented here.

The Aharonov–Bohm effect consists in the scattering of charged particules arriving normally on a whisker of magnetic flux. Classically no effect is expected because the magnetic field vanishes outside the arbitrarily thin solenoid [5]. But not in quantum mechanics: some interferences occur between the parts of the incident plane wave which pass either at the right or at the left of the whisker. And these interferences lead to a non-zero cross section.

This paper describes the scattering of charged particles on a potential of cylindrical symmetry superposed to a whisker of magnetic flux. Two different approaches of the problem will be considered.

First an asymptotic expansion of the solution of the corresponding Schrödinger's equation is calculated in order to find the phase shifts which are composed of two terms. One term represents exactly the Aharonov–Bohm phase

shift obtained by Henneberger [6], while the other one is equal to the phase shift due to the potential but evaluated for a non-integer value of the angular momentum. The fractional part of the angular momentum is proportional to the magnetic flux; so, by varying this flux, the phase shift becomes a function on the full real axis.

In the second approach, the Aharonov–Bohm fiber is removed, but at the same time a canonical transformation introduces some scattering variables (deflection angle, time delay). This transformation is not one-to-one and thus a non-trivial ambiguity group exists. To each irreducible representation of this group corresponds an invariant subspace. The restriction of the scattering operator to such a subspace coincides exactly with the result found in the first approach. Therefore, this restriction reintroduces naturally the Aharonov–Bohm effect, an effect which depends obviously on the chosen subspace. As pointed out by Roy et al. [7] and Ruijsenaars [8] it is important to remark that the operator $i\partial/\partial\theta$ ($\theta \in [0, 2\pi[$) is not essentially self-adjoint. In fact we shall see that the irreducible representations of the ambiguity group are related to the self-adjoint extensions of the operator $i\partial/\partial\theta$.

Finally, an example is presented in the last section. For a particular value of the magnetic flux and for the potential γ/q, the scattering amplitude can be calculated analytically. By changing γ we obtain an interesting comparison between the pure Aharonov–Bohm effect and the scattering on the potential γ/q alone.

Throughout the paper the following conventions will be made:

$$\sum_{l=-\infty}^{\infty} = \sum_{l}, \qquad \int_{-\infty}^{\infty} d\lambda = \int d\lambda.$$

2. Conventional approach

Consider a solenoid along the z axis which is infinitely long, arbitrarily thin, impenetrable, containing a magnetic flux Φ_0, and a potential V of cylindrical symmetry superposed to this whisker. We shall study the quantum scattering of charged particles arriving perpendicularly to the whisker. For such a system the Schrödinger's equation is

$$\frac{1}{2m}\left(\frac{\hbar}{i}\frac{\partial}{\partial\vec{q}} - \frac{e}{c}\vec{A}\right)^2 \psi(\vec{q}) + V\psi(\vec{q}) = E\psi(\vec{q}), \tag{2.1}$$

where $\vec{A}$ describes the whisker:

$$\vec{A} = \frac{\Phi_0}{2\pi q^2}\begin{pmatrix} -q_y \\ q_x \end{pmatrix}, \qquad \vec{q} \in \mathbb{R}^2. \tag{2.2}$$

In cylindrical coordinates $\vec{q} = (q, \theta)$, equation (2.1) reads

$$\left[\frac{\partial^2}{\partial q^2} + \frac{1}{q}\frac{\partial}{\partial q} + \frac{1}{q^2}\left(\frac{\partial}{\partial\theta} + i\alpha\right)^2 + \left(k^2 - \frac{2mV}{\hbar^2}\right)\right]\psi(q, \theta) = 0 \tag{2.3}$$

with $k^2 = 2mE/\hbar^2$ (scattering state) and $\alpha = -e\Phi_0/2\pi\hbar c$. For the sake of simplicity, α is assumed to satisfy the inequalities $0 \leq \alpha < 1$.

Next we expand the wave function ψ in partial waves by choosing the boundary conditions $\psi(\theta = 0) = \psi(\theta = 2\pi)$ which correspond to the conventional

extension of the operator $i\partial/\partial\theta$ used for example by Aharonov and Bohm [9]:

$$\psi = \sum_l e^{il\theta} R_{l+\alpha}(kq), \tag{2.4}$$

where $R_{l+\alpha}$ verifies

$$(kq)^2 R''_{l+\alpha} + kqR'_{l+\alpha} + \left[\left(1-\frac{V}{E}\right)(kq)^2 - (l+\alpha)^2\right] R_{l+\alpha} = 0. \tag{2.5}$$

If the potential V tends sufficiently rapidly to zero as $q \to \infty$, the asymptotic form of $R_{l+\alpha}$ is given by

$$R_{l+\alpha} \sim A_{l+\alpha}\, e^{i\delta_{|l+\alpha|}} [\cos\delta_{|l+\alpha|} J_{|l+\alpha|}(kq) - \sin\delta_{|l+\alpha|} Y_{|l+\alpha|}(kq)], \tag{2.6}$$

where we have used the conventions of Abramowitz and Stegun [10] for the Bessel functions J and Y. The phase shift $\delta_{|l+\alpha|}$ is a functional of the potential determined by the exact radial wave function with the boundary condition $R_{l+\alpha}(0) = 0$ (since the whisker is impenetrable). $A_{l+\alpha}$ is chosen in order to obtain the correct incident plane wave

$$\psi_i = e^{i(kq\cos\theta - \alpha\theta)} \tag{2.7}$$

which gives a constant current density in the positive x direction. The further calculations will show that we have to choose

$$A_{l+\alpha} = \exp\left[-i\left(|l+\alpha|\frac{\pi}{2} + (l+\alpha)\pi\right)\right]. \tag{2.8}$$

It is very useful to separate ψ in two parts, $\psi = \psi_1 + \psi_2$, where

$$\psi_1 = \sum_l e^{il\theta} A_{l+\alpha} J_{|l+\alpha|}(kq) \tag{2.9}$$

and

$$\psi_2 \sim \sum_l e^{il\theta} A_{l+\alpha} [(e^{i\delta_{|l+\alpha|}} \cos\delta_{|l+\alpha|} - 1) J_{|l+\alpha|}(kq) - e^{i\delta_{|l+\alpha|}} \sin\delta_{|l+\alpha|} Y_{|l+\alpha|}(kq)]. \tag{2.10}$$

ψ_1 is the exact Aharonov–Bohm wave function [9], while ψ_2 represents the contribution due to the potential, but modified by the whisker.

Now we have to find the asymptotic form of ψ_1 and ψ_2 in order to have

$$\psi \sim e^{i(kq\cos\theta - \alpha\theta)} + \frac{e^{ikq}}{\sqrt{q}} f(\alpha, \theta). \tag{2.11}$$

The asymptotic expansion of ψ_1 is well-known: for example Berry et al. [11] have proposed an elegant method to get it by using an integral representation for $J_{|l+\alpha|}$ in the complex plane. The result is

$$\psi_1 \sim e^{i(kq\cos\theta - \alpha\theta)} + \frac{e^{ikq}}{\sqrt{q}} \frac{1}{\sqrt{2\pi k}} \exp\left[-i\left(\frac{\pi}{4} + \alpha\pi\right)\right] e^{-i(\theta/2)} \frac{\sin(\alpha\pi)}{\sin\dfrac{\theta}{2}}. \tag{2.12}$$

A straightforward calculation leads to the result

$$\lim_{\varepsilon \to 0} \sum_l e^{il\theta} e^{-|l|\varepsilon} \left[\exp\left[-i\frac{l+\alpha}{|l+\alpha|}\alpha\pi\right] - 1\right] = e^{-i(\theta/2)} \frac{\sin(\alpha\pi)}{\sin\dfrac{\theta}{2}} \tag{2.13}$$

and therefore

$$\psi_1 \sim e^{i(kq\cos\theta-\alpha\theta)}+\frac{e^{ikq}}{\sqrt{q}}\frac{1}{\sqrt{2\pi k}} \times\exp\left[-i\left(\frac{\pi}{4}+\alpha\pi\right)\right]\sum_l e^{il\theta}\left[\exp\left[-i\frac{l+\alpha}{|l+\alpha|}\alpha\pi\right]-1\right] \quad (2.14)$$

where the sum must be understood in the sense of equation (2.13). The linear combination of $J_{|l+\alpha|}$ and $Y_{|l+\alpha|}$ involved in equation (2.10) can be replaced by an Hankel function

$$\psi_2 \sim \tfrac{1}{2}\sum_l e^{il\theta}A_{l+\alpha}\left[e^{i2\delta_{|l+\alpha|}}-1\right]H^{(1)}_{|l+\alpha|}(kq) \quad (2.15)$$

and using the asymptotic behaviour of this Hankel function [10]

$$\psi_2 \sim \frac{e^{ikq}}{\sqrt{q}}\frac{1}{\sqrt{2\pi k}}\exp\left[-i\left(\frac{\pi}{4}+\alpha\pi\right)\right]\sum_l e^{il\theta}\exp\left[-i\frac{l+\alpha}{|l+\alpha|}\alpha\pi\right] \times[e^{i2\delta_{|l+\alpha|}}-1]. \quad (2.16)$$

Finally, adding equation (2.14) and equation (2.16), and comparing with equation (2.11),

$$f(\alpha,\theta)=\frac{1}{\sqrt{2\pi k}}\exp\left[-i\left(\frac{\pi}{4}+\alpha\pi\right)\right] \times\sum_l e^{il\theta}\left[\exp\left[i\left(-\frac{l+\alpha}{|l+\alpha|}\alpha\pi+2\delta_{|l+\alpha|}\right)\right]-1\right]. \quad (2.17)$$

This last expression shows that the phase shift due to the potential adds to the one produced by the whisker. Moreover, by varying from 0 to $-2\pi\hbar c/e$ the flux contained in the whisker, the phase shift δ becomes physically accessible for all real values of the angular momentum. We still remark that for θ different from zero, the equation (2.17) gives the relation

$$f(1-\alpha, 2\pi-\theta)=e^{i(\theta+2\alpha\pi)}f(\alpha,\theta). \quad (2.18)$$

Thus if we know the scattering amplitude for $\theta\in]0,\pi]$ and $\alpha\in[0,1[$, we can deduce it for $\theta\in[\pi,2\pi[$.

In the following section we shall be able to understand better the structure of the S-matrix. In particular we shall see how it depends on terms which represent the orbiting of the particle around the whisker.

3. Geometrical aspect

We first briefly recall the results obtained by us in a previous paper [4], but by introducing them in a slightly different manner. Consider the one-to-one canonical transformation

$$f:\mathbb{R}^2-\{\vec{0}\}\times\mathbb{R}^2-\{\vec{0}\}\to\mathbb{R}\times\mathbb{R}-\{0\}\times[0,2\pi[\times\mathbb{R}^+ \quad (\vec{q},\vec{p})\mapsto(\tau,\lambda;\kappa,\varepsilon) \quad (3.1)$$

defined by

$$\begin{aligned} \tau &= m\frac{\vec{q}\cdot\vec{p}}{p^2} \quad \lambda = q_x p_y - q_y p_x \\ \kappa &= tg^{-1}\frac{p_y}{p_x} \quad \varepsilon = \frac{p^2}{2m}. \end{aligned} \tag{3.2}$$

In order to be able to take $(\tau, \lambda; \kappa, \varepsilon)\times\mathbb{R}\times\mathbb{R}-\{0\}\times\mathbb{R}\times\mathbb{R}-\{0\}$ we have to consider the ambiguity group of f [1, 2, 3]. This group is given by the direct product of $\mathbb{Z}$ with the inversion group $\{\pm 1\}$:

$$[n, j](\tau, \lambda; \kappa, \varepsilon) = (\tau, \lambda; \kappa + 2\pi n, j\varepsilon), \qquad (n, j)\in\mathbb{Z}\times\{\pm 1\}. \tag{3.3}$$

Thus, it is equivalent to know $(\vec{q}, \vec{p}; n, j)$ or $(\tau, \lambda; \kappa, \varepsilon)\in\mathbb{R}\times\mathbb{R}-\{0\}\times\mathbb{R}\times\mathbb{R}-\{0\}$. Now we would like to quantise the transformation f. To this end we define two orthonormal basis of $L^2(\mathbb{R}^2)$ (in Dirac's sense), $|\tau, \lambda\rangle$ and $|\kappa, \varepsilon\rangle$, related by

$$\langle\kappa, \varepsilon \mid \tau, \lambda\rangle = \frac{1}{2\pi\hbar} e^{i/\hbar(\kappa\lambda - \varepsilon\tau)}. \tag{3.4}$$

The operators $(T, L; K, H)$ having respectively $|\tau, \lambda\rangle$ and $|\kappa, \varepsilon\rangle$ as eigenfunctions will be associated to the classical variables $(\tau, \lambda; \kappa, \varepsilon)$, which are also the eigenvalues of these operators. We shall write the momentum operator $\vec{P}$ in cylindrical coordinates by means of K and H:

$$P = \sqrt{2m\,|H|}, \qquad \Phi = K - 2\pi\left[\frac{K}{2\pi}\right] \tag{3.5}$$

where $[x]$ denotes the integer part of x. P and Φ do not represent a complete set of commuting observables in $L^2(\mathbb{R}^2)$. This fact is related with the ambiguity group introduced previously: indeed the unitary operators $\mathscr{A}$ and $\mathscr{P}$,

$$\begin{aligned} \langle\kappa, \varepsilon|\,\mathscr{A}\,|\psi\rangle &= \langle\kappa + 2\pi, \varepsilon \mid \psi\rangle \\ \langle\kappa, \varepsilon|\,\mathscr{P}\,|\psi\rangle &= \langle\kappa, -\varepsilon \mid \psi\rangle \end{aligned} \tag{3.6}$$

commute both with P and Φ. Thus, we can construct a new ket $|p, \varphi; \nu, j\rangle$ $(\nu\in[0, 1[, j\in\{\pm 1\})$

$$\begin{aligned} \langle\kappa, \varepsilon \mid p, \varphi; \nu, j\rangle = \frac{1}{\sqrt{2m}}\Bigg[&\delta\left(\varepsilon - j\frac{p^2}{2m}\right) \\ &+ j\delta\left(\varepsilon + j\frac{p^2}{2m}\right]\delta\left(\kappa - 2\pi\left[\frac{\kappa}{2\pi}\right] - \varphi\right)e^{i2\pi\nu[\kappa/2\pi]} \end{aligned} \tag{3.7}$$

which is eigenfunction of $(P, \Phi; \mathscr{A}, \mathscr{P})$ with eigenvalues $(p, \varphi; e^{i2\pi\nu}, j)$. This ket constitutes a generalisation of the momentum representation and, using the Poisson summation formula, we easily verify that it forms a new orthonormal basis of $L^2(\mathbb{R}^2)$. We remark also that all the irreducible representations of the (abelian) ambiguity group $\mathbb{Z}\times\{\pm 1\}$ are exactly characterised by $\nu\in[0, 1[$ and $j\in\{\pm 1\}$. Moreover, ν has a simple physical signification: by calculating the scalar product $\langle\tau, \lambda \mid p, \varphi; \nu, j\rangle$ we see that it is just equal to the fractional part of the

angular momentum in $\hbar$ units:

$$\langle \tau, \lambda \mid p, \varphi; \nu, j\rangle = \frac{1}{2\pi\hbar}\frac{1}{\sqrt{2m}}\exp\left[-\frac{i}{\hbar}\lambda\varphi\right] \times\left[\exp\left[\frac{i}{\hbar}\tau j\frac{p^2}{2m}\right]+j\exp\left[-\frac{i}{\hbar}\tau j\frac{p^2}{2m}\right]\right]\delta\left(\frac{\lambda}{\hbar}-\left[\frac{\lambda}{\hbar}\right]-\nu\right). \quad (3.8)$$

In addition from equation (3.7) we remark:

$$\langle \kappa+2\pi, \varepsilon \mid p, \varphi; \nu, j\rangle = e^{i2\pi\nu}\langle \kappa, \varepsilon \mid p, \varphi; \nu, j\rangle. \quad (3.9)$$

This relation is identical to the formula (14) of [7]; hence ν fixes at the same time the self-adjoint extensions of the operator $i\partial/\partial\theta$.

With the variables $(\tau, \lambda; \kappa, \varepsilon)$ we would like to study the scattering of particles by a potential of cylindrical symmetry.

Classically the S-matrix applies canonicaly the straight line $(\tau, \lambda; \kappa, \varepsilon)$ on the straight line $(\tau', \lambda; \kappa', \varepsilon)$ ($(\lambda, \kappa, \varepsilon)$ and $(\lambda, \kappa', \varepsilon)$ determine the asymptotes of the motion while τ and τ' fix a point on them). It is described by the generating function

$$G(\kappa', \varepsilon'; \tau, \lambda) = \kappa'\lambda - \varepsilon'\tau - 2\pi\lambda\theta(\lambda) + 2\hbar\delta_{|\lambda|}(|\varepsilon'|) \quad (3.10)$$

where $\hbar\delta_{|\lambda|}(|\varepsilon'|)$ is the classical phase shift [12]. If we differentiate G, the time delay and the deflection angle are obtained:

$$\tau' - \tau = -2\hbar\frac{\partial}{\partial\varepsilon'}\delta_{|\lambda|}(|\varepsilon'|), \qquad \kappa' - \kappa = 2\pi\theta(\lambda) - 2\hbar\frac{\partial}{\partial\lambda}\delta_{|\lambda|}(|\varepsilon'|). \quad (3.11)$$

To understand the term $2\pi\theta(\lambda)$ in equation (3.11) we recall that the direction of the incident particle is determined by $\vec{p}$, while $\vec{p}' = p(\vec{q}'/q')$ $(q' \to \infty)$ gives the outgoing asymptote. Now it is sufficient to consider free particles: figure 1 shows that the deflection angle is either 0 or 2π and thus it depends on the sign of the angular momentum, which agrees with equation (3.11). In quantum mechanics we propose the following expression for the S-matrix:

$$\langle \kappa', \varepsilon' \mid S \mid \tau, \lambda\rangle = \frac{1}{2\pi h}\exp\left[\frac{i}{\hbar}(\kappa'\lambda - \varepsilon'\tau - 2\pi\lambda\theta(\lambda) + 2\hbar\delta_{|\lambda|}(|\varepsilon'|))\right] \quad (3.12)$$

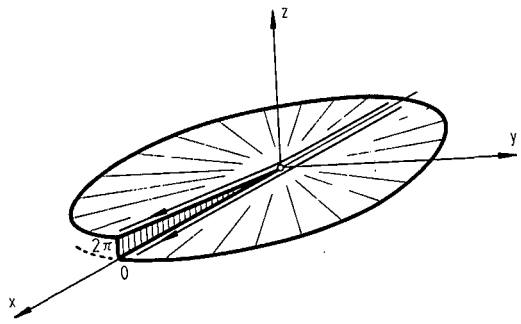

Figure 1
Classical trajectories for free particles showing that the deflection angle depends on the sign of the angular momentum: $\kappa' - \kappa = 2\pi\theta(\lambda)$

where δ has to be calculated now from the Schrödinger's equation. This form is chosen in order to correspond to an unitary operator and to reduce to the generating function (3.10) in the semi-classical approximation. In a real scattering experiment an incident plane wave (given by $\vec{p}$) is sent on the target and a scattered wave is detected in the direction fixed by $\vec{p}'$. Therefore, the interesting S-matrix elements are $\langle p', \varphi'; \nu', j' | S | p, \varphi; \nu, j \rangle$. From equation (3.12) a short calculation shows that S commutes with the ambiguity operators $\mathscr{A}$ and $\mathscr{P}$. So we have

$$\langle p', \varphi'; \nu', j' | S | p, \varphi; \nu, j \rangle = \frac{1}{p} \delta(p'-p)\delta(\nu'-\nu)\delta_{j'j} S\nu(\varphi', \varphi). \tag{3.13}$$

From a mathematical point of view the S-matrix has been defined on the sheeted phase space $(\kappa, \varepsilon; \tau, \lambda)$ by equation (3.12). Thus, we can consider equation (3.13) as the restrictions of the scattering operator to the subspaces labelled by the indices (ν, j) which distinguish the irreducible representations of the ambiguity group.

Making use of the completeness relations

$$\iint d\kappa\, d\varepsilon\, |\kappa, \varepsilon\rangle\langle\kappa, \varepsilon| = \iint d\tau\, d\lambda\, |\tau, \lambda\rangle\langle\tau, \lambda| = \mathbb{1} \tag{3.14}$$

$S\nu(\varphi', \varphi)$ reads:

$$S\nu(\varphi', \varphi) = \frac{1}{2\pi\hbar} \sum_n \int d\lambda \exp\left[i2\pi n\left(\nu - \frac{\lambda}{\hbar}\right)\right] \times \exp\left[\frac{i}{\hbar}\left[(\varphi'-\varphi)\lambda - 2\pi\lambda\theta(\lambda) + 2\hbar\delta_{|\lambda|}\left(\frac{p^2}{2m}\right)\right]\right]. \tag{3.15}$$

And finally, again with the Poisson summation formula, we obtain

$$S\nu(\varphi', \varphi) = \frac{1}{2\pi} e^{i\nu(\varphi'-\varphi-\pi)} \sum_l e^{il(\varphi'-\varphi)} \times \exp\left[i\left(-\frac{l+\nu}{|l+\nu|}\nu\pi + 2\delta_{|l+\nu|}\left(\frac{p^2}{2m}\right)\right)\right]. \tag{3.16}$$

Now comes the most important step of this paper: the comparison of the two expressions (2.17) and (3.16). For θ different from zero S_ν is proportional to f if the following choices are made: $\nu \equiv \alpha$ and $\theta \equiv \varphi' - \varphi$. From these identifications we see that the S-matrix (3.12) describes exactly the scattering by a whisker of magnetic flux and a potential, although the whisker was not introduced explicitly in equation (3.12)! The effect due to the solenoid depends on the subspace (ν, j) which is chosen to project the S-matrix. More precisely, in absence of the potential (i.e. when all the phase shifts are zero) the S-matrix (3.12) do not reduce to the identity operator. In this case only its restriction to the subspace $\nu = 0$ equals the identity operator, while its other restrictions give a pure Aharonov–Bohm scattering.

In order to understand better the final formula (3.16) we shall still note that the expression (3.15) is particularly convenient to make a semi-classical approximation. If we apply the stationary phase method to each term of equation (3.15),

we have to find some λ which verify

$$\varphi' - \varphi = 2\pi n + 2\pi\theta(\lambda) - 2\hbar \frac{\partial}{\partial \lambda} \delta_{|\lambda|}\left(\frac{p^2}{2m}\right). \tag{3.17}$$

So the nth term represents the probability amplitude to detect the scattered particule after an orbiting of n turns around the whisker. And because the particle entwines n times the flux of the solenoid the total phase is modified by the value of $2\pi n\nu$ (see equation (3.15)).

4. An example

It is well known that an analytic expression for the scattering amplitude can be found for the potential γ/q. In this section we shall show that the same calculations are always possible if a whisker containing a flux $-\pi\hbar c/e$ is added to the potential. To this flux corresponds a flux parameter α equal to one half, which leads to a maximum Aharonov–Bohm cross-section (see equation (2.12)).

For θ different from zero, the equation (2.17) gives

$$f(\tfrac{1}{2}, \theta) = -\frac{1}{\sqrt{2\pi k}} e^{i(\pi/4)} \sum_l e^{il\theta} \exp\left[i\left(-\frac{l+\frac{1}{2}}{|l+\frac{1}{2}|}\frac{\pi}{2} + 2\delta_{|l+\frac{1}{2}|}\right)\right] \tag{4.1}$$

$$f(\tfrac{1}{2}, \theta) = -\frac{2}{\sqrt{2\pi k}} e^{i(\pi/4)} e^{-i(\theta/2)} \sum_0^\infty \exp\left[i2\delta_{|l+\frac{1}{2}|}\right] \sin\left(l+\tfrac{1}{2}\right)\theta. \tag{4.2}$$

In our example, the phase shifts $\delta_{|l|}$ have to be determined from the Schrödinger's equation

$$\Delta\psi + \left(k^2 - \frac{2m\gamma}{\hbar^2}\frac{1}{q}\right)\psi = 0. \tag{4.3}$$

We verify easily that the regular solution at the origin reads

$$\psi = \sum_l C_l e^{il\theta} e^{ikq} q^{|l|} M\left(|l|+\tfrac{1}{2}+i\frac{m\gamma}{\hbar^2 k}, 2|l|+1; -2ikq\right) \tag{4.4}$$

where M denotes the confluent hypergeometric function. Using the asymptotic expansion for M[10], we obtain the phase shifts:

$$e^{i2\delta_{|l|}} = \frac{\Gamma\left(|l|+\frac{1}{2}+i\frac{m\gamma}{\hbar^2 k}\right)}{\Gamma\left(|l|+\frac{1}{2}-i\frac{m\gamma}{\hbar^2 k}\right)}. \tag{4.5}$$

Evaluating these phase shifts at $|l+\frac{1}{2}|$ rather than at $|l|$, we find an explicit formula for the scattering amplitude (4.2):

$$f(\tfrac{1}{2}, \theta) = -\frac{2}{\sqrt{2\pi k}} e^{i(\pi/4)} e^{-i(\theta/2)} \sum_0^\infty \frac{\Gamma\left(l+1+i\frac{m\gamma}{\hbar^2 k}\right)}{\Gamma\left(l+1-i\frac{m\gamma}{\hbar^2 k}\right)} \sin\left(l+\tfrac{1}{2}\right)\theta. \tag{4.6}$$

But this last sum is proportional to the trigonometric expansion of a Legendre function [10], so

$$f(\tfrac{1}{2}, \theta) = -\frac{1}{\sqrt{2k}} e^{i(\pi/4)} 2^{-\mu} \Gamma(\mu + \tfrac{1}{2}) e^{-i(\theta/2)} \left(\sin\frac{\theta}{2}\right)^{-\mu} P^{\mu}_{-\mu}\left(\cos\frac{\theta}{2}\right), \qquad \mu = \tfrac{1}{2} + i\frac{m\gamma}{\hbar^2 k}. \tag{4.7}$$

Next, we remark that the function $P^{\mu}_{-\mu}$ can be expressed by means of a more elementary function:

$$f(\tfrac{1}{2}, \theta) = -\frac{1}{\sqrt{2k}} e^{i(\pi/4)} \frac{\Gamma\left(1 + i\frac{m\gamma}{\hbar^2 k}\right)}{\Gamma\left(\frac{1}{2} - i\frac{m\gamma}{\hbar^2 k}\right)} \frac{e^{-i(\theta/2)}}{\sin\frac{\theta}{2}} \left(\sin\frac{\theta}{2}\right)^{-i(2m\gamma/\hbar^2 k)} \tag{4.8}$$

And finally, separating modulus and phase

$$|f(\tfrac{1}{2}, \theta)|^2 = \frac{\gamma}{4E} \frac{1}{\sin^2\frac{\theta}{2}} \operatorname{cth} \frac{\pi m\gamma}{\hbar\sqrt{2mE}} \tag{4.9}$$

$$\arg f(\tfrac{1}{2}, \theta) = \frac{5\pi}{4} - \frac{\theta}{2} - \frac{2m\gamma}{\hbar\sqrt{2mE}} \ln\left(\sin\frac{\theta}{2}\right) + \arg\Gamma\left(1 + i\frac{m\gamma}{\hbar\sqrt{2mE}}\right) - \arg\Gamma\left(\tfrac{1}{2} - i\frac{m\gamma}{\hbar\sqrt{2mE}}\right). \tag{4.10}$$

This scattering amplitude possesses the following properties:

i) The change of sign of γ affects only the phase (4.10).

ii) If both $\hbar$ and Φ_0 tend to zero in such a way that the flux parameter α remains equal to one half, then $|f|^2$ approaches the classical cross section due to the potential γ/q:

$$|f(\tfrac{1}{2}, \theta)|^2 = \frac{|\gamma|}{4E} \frac{1}{\sin^2\frac{\theta}{2}}. \tag{4.11}$$

iii) The limit $\gamma = 0$ leads naturally to a pure Aharonov–Bohm scattering:

$$|f(\tfrac{1}{2}, \theta)|^2 = \frac{\hbar}{2\pi\sqrt{2mE}} \frac{1}{\sin^2\frac{\theta}{2}}. \tag{4.12}$$

iv) Inversely, for $|\gamma|$ which goes to infinity, only γ/q contributes to $|f|^2$; in this case $|f|^2$ equals again the classical cross section (4.11).

Now we understand why this example can be solved completely in an analytic way: the scattering on the potential γ/q and the Aharonov–Bohm scattering give some proportional cross sections. And if both interactions are present, the factor

$$\operatorname{cth} \frac{\pi m\gamma}{\hbar\sqrt{2mE}} \tag{4.13}$$

in equation (4.9) leads to the correct cross section.

We have also to remark that in the limits ii) and iv) the Aharonov–Bohm effect subsists in the phase (4.10):

$$\arg f(\tfrac{1}{2}, 2\pi - \theta) = \arg f(\tfrac{1}{2}, \theta) + \theta - \pi. \tag{4.14}$$

But unfortunately this phase remains inaccessible to the experience!

5. Conclusion

In this paper we have given a geometrical (group-theoretical) interpretation of the Aharonov–Bohm effect.

The crucial point of the above considerations consists in the introduction of the ambiguity group to which are associated the variables 'deflection angle' and 'time delay'; in fact this group reflects the topological structure of the phase space. In this frame it should be certainly interesting to analyse the situation where the configuration space is bored by more than one solenoid.

As pointed out recently by Amiet and Huguenin [13, 14], we remark that the concept of generating functions clarifies certain analogies between the classical and quantum mechanics. We shall note particularly the similitude between the formulas (3.10) and (3.12) and the possibility to make a semi-classical approximation with equation (3.15).

In a next stage we think to replace the cylindrical potential by a spherical potential to treat the three-dimensional scattering. In order to use the formalism developed in this paper, the spherical harmonics have to be generalised for non-integer indices.

REFERENCES

[1] M. MOSHINSKY and T. H. SELIGMAN, Ann. of Phys. (N.Y.), *114*, 243 (1978).
[2] M. MOSHINSKY and T. H. SELIGMAN, Ann. of Phys. (N.Y.), *120*, 402 (1979).
[3] M. MOSHINSKY and T. H. SELIGMAN, Ann. of Phys. (N.Y.), *127*, 458 (1980).
[4] F. GUILLOD and P. HUGUENIN, J. Phys., A15, 3705 (1982).
[5] W. C. HENNEBERGER and P. HUGUENIN, Helv. Phys. Acta, *54*, 444 (1981).
[6] W. C. HENNEBERGER, Phys. Rev., *A22*, 1383 (1980).
[7] S. ROY and V. SINGH, *Time Dependent Aharonov–Bohm Hamiltonian and admissability criteria of quantum wave function* (Preprint: October 1982).
[8] S. RUIJSENAARS, Ann. of Phys. (N.Y.), *146*, 1 (1983).
[9] Y. AHARONOV and D. BOHM, Phys. Rev., *115*, 485 (1959).
[10] M. ABRAMOWITZ and I. STEGUN, *Handbook of Mathematical Functions* (New-York: Dover) (1964).
[11] M. V. BERRY, R. G. CHAMBERS, M. D. LARGE, C. UPSTILL and J. C. WALMSLEY, Eur. J. Phys., *1*, 154, (1980).
[12] H. NARNHOFER and W. THIRRING, Phys. Rev., *A23*, 1688 (1981).
[13] J.-P. AMIET and P. HUGUENIN, Helv. Phys. Acta, *53*, 377 (1980).
[14] J.-P. AMIET and P. HUGUENIN, Helv. Phys. Acta, *55*, 278 (1982).

J. Phys. A: Math. Gen. 15 (1982) 3705–3714. Printed in Great Britain

Canonical scattering transformation in quantum mechanics

F Guillod and P Huguenin

Institut de Physique, Université de Neuchâtel, Switzerland

Received 20 April 1982

Abstract. We quantise the classical canonical scattering transformation of Hunziker with the representation method of Moshinsky and Seligmann. This leads to a sheeted phase space characterised by the number of turns around the scatterer. The usual detection device projects on the trivial representation of the corresponding ambiguity group. This operation extracts the integer values of the angular momentum.

1. Introduction

Recently, following an idea of Hunziker (1968), Narnhofer and Thirring (1981) have proposed a nice classical picture of the S-matrix theory. In this approach the pertinent object is a generating function of the canonical map between the straight asymptotic trajectories before and after the collision. This generating function is simply twice the phase shift multiplied by $\hbar$.

The concept of generating functions of canonical transformations is old and forgotten among the physicist community. A new look at the geometrical significance of this formalism may be found in Amiet and Huguenin (1980) for example. The use of these generating functions for the calculation of matrix elements of unitary transformations (Amiet and Huguenin 1981) enhances its significance for quantum mechanics as already seen by Van Vleck (1928).

The quantisation of the classical result of Narnhofer and Thirring is, nevertheless, non-trivial. For example the phaseshifts are usually defined for integer values of the angular momentum, and the definition of the derivative is ambiguous, i.e. the deflection angle is not properly defined in quantum mechanics.

The reason for the difficulty is that the appropriate variables for the description of the scattering are the action-angle variables related to the conserved quantities instead of the original (q, p) phase space variables, a transformation which is not one-to-one.

A way to solve this kind of problem may be found in the work of Moshinsky and Seligmann (1980). The concept of ambiguity of a canonical transformation finds a natural application in the domain of scattering. Roughly speaking, the detector does not separate the contributions of the number of turns of the projectile around the scatterer. This is the physical ambiguity. The detector is sensitive to the coherent sum of contributions of an arbitrary number of turns. The result is a projection onto the trivial representation of the ambiguity group. This projection retains only the integer values of the angular momentum. In the discussion of Aharonov–Bohm scattering, Berry (1980) has already proposed a similar approach.

0305-4470/82/123705+10$02.00

In this paper, we deal with scattering in the plane by a central potential with all conditions guaranteeing the existence of the asymptotic states. We use the following conventions:

$$\sum_{l=-\infty}^{\infty} = \sum_{l} \qquad \int_{-\infty}^{\infty} d\lambda = \int d\lambda.$$

2. Classical scattering

Here we recall the results of Narnhofer and Thirring (1981) with special emphasis on the ambiguity related to the use of polar coordinates in the momentum plane. Consider the map

$$f: \mathbb{R}^2 \times \mathbb{R}^2 \to \mathbb{R} \times \mathbb{R} \times [0, 2\pi[\times \mathbb{R}^+$$
$$(q, p) \mapsto (t, \mathscr{L}; \chi, h)$$

defined by (figure 1)

$$t = m\, q \cdot p / \|p\|^2 \qquad \mathscr{L} = q_x p_y - q_y p_x \qquad \chi = \tan^{-1} p_y/p_x \qquad h = \|p\|^2/2m. \quad (2.1)$$

Except for $\|p\| = 0$, the mapping exists and is one-to-one. But for the sake of quantisation, the edge of the domain of $(t, \mathscr{L}; \chi, h)$ presents some difficulties. Following Moshinsky and Seligmann (1977, 1979, 1980), we propose to extend the mapping f continuously in such a way that $(t, \mathscr{L}; \chi, h) \in \mathbb{R}^4$. To this end, we define the domains D_N which cover $\mathbb{R}^4$:

$$D_N = \mathbb{R} \times \mathbb{R} \times [N\pi, (N+2)\pi[\times (-1)^N \mathbb{R}^+ \qquad N \in \mathbb{Z}.$$

The mapping

$$a: D_N \to D_{N+1}$$
$$(t, \mathscr{L}; \chi, h) \mapsto (-t, \mathscr{L}; \chi + \pi, -h) \quad (2.2)$$

generates the group $\mathbb{Z}$ and the powers of a relate the D_N to one another. It follows

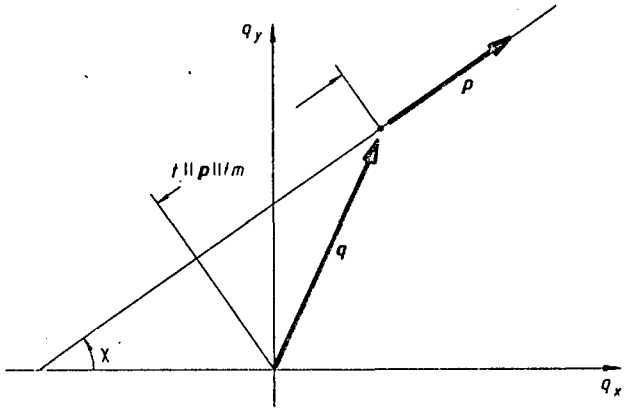

Figure 1. $(t, \mathscr{L}; \chi, h)$ are the appropriate variables for the description of the scattering, in particular for the time delay and the deflection angle.

that for all $(t, \mathscr{L}; \chi, h) \in \mathbb{R}^4$ there exists one (unique) $N \in \mathbb{Z}$ such that

$$a^{-N}(t, \mathscr{L}; \chi, h) \in D_0$$

(provided simply that $h \neq 0$). We propose now an extension F of f by introducing a sheeted phase space

$$F : \mathbb{Z} \times \mathbb{R}^2 \times \mathbb{R}^2 \to \mathbb{R}^4 \qquad (N, \boldsymbol{q}, \boldsymbol{p}) \mapsto (t, \mathscr{L}; \chi, h) \in D_N$$

with

$$t = (-1)^N m\boldsymbol{q} \cdot \boldsymbol{p}/\|\boldsymbol{p}\|^2 \qquad \mathscr{L} = q_x p_y - q_y p_x \qquad \chi = \tan^{-1} p_y/p_x + N\pi$$
$$h = (-1)^N \|\boldsymbol{p}\|^2/2m. \tag{2.3}$$

The inverse transformation F^{-1} is given by

$$q_x = \frac{(-1)^N}{\sqrt{(-1)^N 2mh}}(2th \cos\chi + \mathscr{L} \sin\chi) \qquad p_x = (-1)^N \sqrt{(-1)^N 2mh} \cos\chi$$

$$q_y = \frac{(-1)^N}{\sqrt{(-1)^N 2mh}}(2th \sin\chi - \mathscr{L} \cos\chi) \qquad p_y = (-1)^N \sqrt{(-1)^N 2mh} \sin\chi$$

with N such that

$$(-1)^N = h/|h| \qquad \chi - N\pi \in [0, 2\pi[.$$

In this way we achieve a covering of $\mathbb{R}^2 \times \mathbb{R}^2$ where the subspace $\mathbb{R}^2 \times \{\mathbf{0}\}$ is removed or, inversely, we cover $\mathbb{R}^4$ with an infinity of mappings of $\mathbb{R}^2 \times \mathbb{R}^2$ (figure 2).

The transformation F is canonical and one of its generating functions reads

$$W(p_x, p_y; t, \mathscr{L}) = \mathscr{L}(\tan^{-1} p_y/p_x + N\pi) - (-1)^N t(p_x^2 + p_y^2)/2m. \tag{2.4}$$

It means

$$q_x = -\partial W/\partial p_x \qquad q_y = -\partial W/\partial p_y \qquad \chi = \partial W/\partial \mathscr{L} \qquad h = -\partial W/\partial t$$

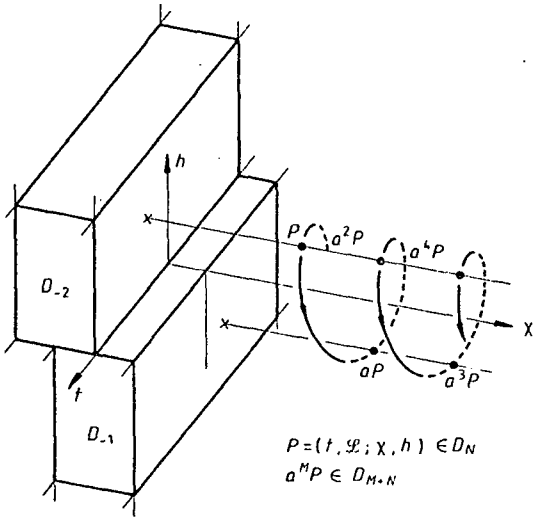

Figure 2. With the generator a, D_N is transformed into D_{N+1} by a translation of π along the χ axis and a rotation of π about the same axis.

and it is simple to calculate the Jacobian

$$\det\begin{pmatrix}\partial^2 W/\partial p_x \partial \mathscr{L} & \partial^2 W/\partial p_x \partial t \\ \partial^2 W/\partial p_y \partial \mathscr{L} & \partial^2 W/\partial p_y \partial t\end{pmatrix} = \frac{(-1)^N}{m} \neq 0$$

which says that W unfolds globally the transformation F.

In the new coordinates the canonical S transformation is very simple. It transforms the straight line $(t, \mathscr{L}; \chi, h)$, $-\infty < t < +\infty$, into the new straight line $(t', \mathscr{L}'; \chi', h')$, $-\infty < t' < +\infty$, canonically, where $h' = h$ and $\mathscr{L}' = \mathscr{L}$ with our hypothesis on the potential.

The transformation is like a gauge transformation in the energy–angular-momentum variables, and the corresponding generating function reads

$$G(t', \mathscr{L}'; \chi, h) = \chi \mathscr{L}' - ht' + 2\hbar \delta_{\mathscr{L}'}(|h|) \tag{2.5}$$

with

$$t = -\partial G/\partial h \qquad \mathscr{L} = \partial G/\partial \chi \qquad \chi' = \partial G/\partial \mathscr{L}' \qquad h' = -\partial G/\partial t'$$

where $\delta_{\mathscr{L}'}(|h|)$ is a functional of the scattering potential, as explicitly given by Narnhofer and Thirring. The derivative $2\hbar\, \partial\delta/\partial h$ is the time delay and $2\hbar\, \partial\delta/\partial \mathscr{L}'$ the deflection angle. This angle may be bigger than 2π in the case of orbiting.

3. Quantisation

Before quantising the classical variables $(t, \mathscr{L}; \chi, h)$, we have to choose a Hilbert space. Because $(t, \mathscr{L}; \chi, h) \in \mathbb{R}^4$, we suggest to work with

$$\mathscr{H} = L^2(\mathbb{R}^2, \mathrm{d}\kappa\, \mathrm{d}\varepsilon; \mathbb{C}).$$

We define the $|\kappa, \varepsilon\rangle$ representation of $\mathscr{H}$ by

$$\langle \kappa, \varepsilon | \kappa', \varepsilon' \rangle = \delta(\kappa - \kappa')\delta(\varepsilon - \varepsilon') \tag{3.1a}$$

$$\iint \mathrm{d}\kappa\, \mathrm{d}\varepsilon\, |\kappa, \varepsilon\rangle\langle \kappa, \varepsilon| = \mathbb{1} \tag{3.1b}$$

so that $|\kappa, \varepsilon\rangle$ form an orthonormal basis of $\mathscr{H}$ in Dirac's sense. The $|\tau, \lambda\rangle$ representation of $\mathscr{H}$ is given by

$$\langle \kappa, \varepsilon | \tau, \lambda \rangle = \frac{1}{2\pi\hbar} \exp\left[(\mathrm{i}/\hbar)(\kappa\lambda - \varepsilon\tau)\right] \tag{3.2}$$

in the (3.1) representation. We again have orthogonality and completeness:

$$\langle \tau, \lambda | \tau', \lambda' \rangle = \delta(\tau - \tau')\delta(\lambda - \lambda') \tag{3.3a}$$

$$\iint \mathrm{d}\tau\, \mathrm{d}\lambda\, |\tau, \lambda\rangle\langle \tau, \lambda| = \mathbb{1}. \tag{3.3b}$$

It is interesting to compare the 'plane' wave (3.2) in the angle and time variables with (2.5). The phase of the unitary kernel (3.2) has the Van Vleck form corresponding to the generating function (2.5) if the scattering potential is zero, i.e. for $\delta_{\mathscr{L}'}(|h|) = 0$. Hence for this transformation, the WKB form is exact.

The quantisation of the classical quantities $(t, \mathscr{L}; \chi, h)$ is now possible. We associate the operators $(T, L; K, H)$ to them. They act on $\mathscr{H}$ and in the $|\kappa, \varepsilon\rangle$ representation

they are defined by

$$\begin{aligned} \langle\kappa, \varepsilon|T|\psi\rangle &= \mathrm{i}\hbar \frac{\partial}{\partial\varepsilon}\langle\kappa, \varepsilon|\psi\rangle & \langle\kappa, \varepsilon|L|\psi\rangle &= -\mathrm{i}\hbar \frac{\partial}{\partial\kappa}\langle\kappa, \varepsilon|\psi\rangle \\ \langle\kappa, \varepsilon|K|\psi\rangle &= \kappa\langle\kappa, \varepsilon|\psi\rangle & \langle\kappa, \varepsilon|H|\psi\rangle &= \varepsilon\langle\kappa, \varepsilon|\psi\rangle. \end{aligned} \tag{3.4}$$

Because $(\kappa, \varepsilon) \in \mathbb{R}^2$, $(T, L; K, H)$ are self-adjoint and have a continuous real spectrum. Moreover, $|\kappa, \varepsilon\rangle$ are eigenfunctions of (K, H) and writing (3.4) in the $|\tau, \lambda\rangle$ representation we see that the $|\tau, \lambda\rangle$ are eigenfunctions of (T, L). We can also control that

$$[T, H] = [K, L] = \mathrm{i}\hbar$$

and that all the other commutators vanish.

Now, we should like to describe the number of turns of the projectile around the scatterer. To this end, we define three new operators

$$N = 2[K/2\pi]\theta(H) + (2[(K+\pi)/2\pi] - 1)\theta(-H) \tag{3.5a}$$

$$P = \sqrt{2m|H|} \tag{3.5b}$$

$$\Phi = K - N\pi \tag{3.5c}$$

where $[x]$ denotes the integer part of x.

The operator N will be very useful for the description of a possible orbiting around the potential. Clearly, (P, Φ, N) form a complete set of commuting observables and their eigenfunctions $|p, \varphi, n\rangle$ are given by

$$\langle\kappa, \varepsilon|p, \varphi, n\rangle = m^{-1/2}\delta(\varepsilon - (-1)^n p^2/2m)\delta(\kappa - \varphi - n\pi) \tag{3.6a}$$

$$\langle\tau, \lambda|p, \varphi, n\rangle = \frac{1}{2\pi\hbar}\frac{1}{\sqrt{m}}\exp\{-(\mathrm{i}/\hbar)[\lambda(\varphi + n\pi) - (-1)^n \tau p^2/2m]\}. \tag{3.6b}$$

The range of the spectrum of (P, Φ, N) is $\mathbb{R}^+ \times [0, 2\pi[\times \mathbb{Z}$, so the states $|p, \varphi, n\rangle$ represent a generalisation of the momentum representation. Again the phase of (3.6*b*) is a generating function, namely identical with (2.4). The $|p, \varphi, n\rangle$ representation constitutes a new orthonormal complete set, i.e.

$$\langle p, \varphi, n|p', \varphi', n'\rangle = p^{-1}\delta(p - p')\delta(\varphi - \varphi')\delta_{nn'} \tag{3.7a}$$

$$\sum_n \int_0^\infty p\,\mathrm{d}p \int_0^{2\pi} \mathrm{d}\varphi\, |p, \varphi, n\rangle\langle p, \varphi, n| = \mathbb{1}. \tag{3.7b}$$

To prove (3.7*a*) we use the partition of the identity (3.1*b*)

$$\begin{aligned} \langle p, \varphi, n|p', \varphi', n'\rangle &= \frac{1}{m}\iint \mathrm{d}\kappa\, \mathrm{d}\varepsilon\, \delta\left(\varepsilon - (-1)^n \frac{p^2}{2m}\right) \\ &\quad \times \delta\left(\varepsilon - (-1)^{n'} \frac{p'^2}{2m}\right) \delta(\kappa - \varphi - n\pi)\delta(\kappa - \varphi' - n'\pi) \\ &= \frac{1}{m}\delta\left(\frac{p^2}{2m} - \frac{p'^2}{2m}\right)\delta(\varphi - \varphi')\delta_{nn'} \\ &= \frac{1}{p}\delta(p - p')\delta(\varphi - \varphi')\delta_{nn'} \end{aligned}$$

since $(\varphi, \varphi') \in [0, 2\pi[$, $(p, p') \in \mathbb{R}^+$.

The completeness relation may be verified by taking matrix elements of (3.7*b*):

$$\begin{aligned}\langle\kappa,\varepsilon|\sum_n\int_0^\infty p\,\mathrm{d}p\int_0^{2\pi}\mathrm{d}\varphi\,|p,\varphi,n\rangle\langle p,\varphi,n|\kappa',\varepsilon'\rangle&\\ =\frac{1}{m}\sum_n\int_0^\infty p\,\mathrm{d}p\int_0^{2\pi}\mathrm{d}\varphi\,\delta\left(\varepsilon-(-1)^n\frac{p^2}{2m}\right)\delta\left(\varepsilon'-(-1)^n\frac{p^2}{2m}\right)&\\ \times\delta(\kappa-\varphi-n\pi)\delta(\kappa'-\varphi-n\pi)&\\ =\iint\mathrm{d}x\,\mathrm{d}y\,\delta(\varepsilon-x)\delta(\varepsilon'-x)\delta(\kappa-y)\delta(\kappa'-y)&\\ =\delta(\kappa-\kappa')\delta(\varepsilon-\varepsilon').&\end{aligned}$$

The above calculations exhibit an isomorphism between $\mathscr{H}$ and

$$\mathscr{H}=l^2(\mathbb{Z};L^2(\mathbb{R}^+\times[0,2\pi[,p\,\mathrm{d}p\,\mathrm{d}\varphi;\mathbb{C}))$$

which is suitable for the description of the orbiting.

In fact, $|p,\varphi,n\rangle$ is a 'basis' of $\mathscr{H}$ and the unitary operator $\mathscr{U}$ defined by $\mathscr{U}|\kappa,\varepsilon\rangle=|p,\varphi,n\rangle$ transforms a 'basis' of $\mathscr{H}$ in a 'basis' of $\mathscr{K}$.

To describe the classical mapping a, we introduce the shift operator A defined by

$$\langle p,\varphi,n|A|\psi\rangle=\langle p,\varphi,n+1|\psi\rangle. \tag{3.8}$$

This operator is obviously unitary because $n\in\mathbb{Z}$. Using the partitions of the identity (3.1*b*) and (3.3*b*) we find also

$$\langle\kappa,\varepsilon|A|\psi\rangle=\langle\kappa+\pi,-\varepsilon|\psi\rangle\qquad\langle\tau,\lambda|A|\psi\rangle=\mathrm{e}^{\mathrm{i}\lambda\pi/\hbar}\langle-\tau,\lambda|\psi\rangle. \tag{3.9}$$

We have now introduced all the mathematical formalism needed later about the Hilbert space. The reader could skip directly to § 4.

However, conceptually, we have also to discuss the configuration space. Here we encounter the difficulty that operators $\boldsymbol{Q}$ and N fail to commute. Following ideas suggested by the work of Zak (1968) we can take $\boldsymbol{Q}$ and A as a system of commuting operators. We define the $|q,\nu\rangle$ representation by

$$\begin{aligned}&\langle p,\varphi,n|q,\nu\rangle=\frac{1}{2\pi\hbar}\exp\left[-(\mathrm{i}/\hbar)p(q_x\cos\varphi+q_y\sin\varphi)\right]\exp(\mathrm{i}2\pi\nu n)\\ &(q,\nu)\in\mathbb{R}^2\times[0,1[\end{aligned} \tag{3.10}$$

having the properties

$$\langle q,\nu|q',\nu'\rangle=\delta(q-q')\delta(\nu-\nu') \tag{3.11a}$$

$$\iint\mathrm{d}^2q\int_0^1\mathrm{d}\nu|q,\nu\rangle\langle q,\nu|=\mathbb{1}. \tag{3.11b}$$

We shall prove only (3.11*a*); with (3.7*b*) we obtain

$$\langle q, \nu|q', \nu'\rangle = \frac{1}{(2\pi\hbar)^2}\int_0^\infty p\,\mathrm{d}p\int_0^{2\pi}\mathrm{d}\varphi\,\exp\{(\mathrm{i}/\hbar)p\,[\cos\varphi(q_x - q'_x) + \sin\varphi(q_y - q'_y)]\}\sum_n \exp[\mathrm{i}2\pi n(\nu' - \nu)]$$

$$= \delta(q - q')\sum_n \delta(\nu - \nu' + n)$$

$$= \delta(q - q')\delta(\nu - \nu')$$

where we have used the Poisson formula (A2) and $(\nu, \nu') \in [0, 1[$.

So, in the $|q, \nu\rangle$ representation A is diagonal: using (3.8) and (3.10) we obtain

$$\langle q, \nu|A|\psi\rangle = \mathrm{e}^{\mathrm{i}2\pi\nu}\langle q, \nu|\psi\rangle \tag{3.12}$$

which shows that $\mathrm{e}^{\mathrm{i}2\pi\nu}$ is an eigenvalue of A.

Using (3.12) and (3.9) we obtain

$$\langle q, \nu|A^2|\tau, \lambda\rangle = \exp(\mathrm{i}2\pi 2\nu)\langle q, \nu|\tau, \lambda\rangle = \exp(\mathrm{i}2\pi\lambda/\hbar)\langle q, \nu|\tau, \lambda\rangle.$$

This means that, if the matrix elements are different from zero, then $2\nu - \lambda/\hbar$ has to be an integer. In other words, 2ν is related to the fractional part of the angular momentum in $\hbar$ units.

This achieves the complete analogy between classical and quantum descriptions. The eigenvalues $(\tau, \lambda; \kappa, \varepsilon)$ correspond to the classical variables $(t, \mathscr{L}; \chi, h)$ in the same sense as the eigenvalues of $(\boldsymbol{Q}, \boldsymbol{P})$ correspond to classical variables (q, p).

4. *S*-matrix elements and scattering amplitude

The so-called S matrix is a unitary operator which relates the asymptotic free states before and after the collision. The matrix elements may always be written

$$\langle \kappa, \varepsilon|S|\tau, \lambda\rangle = \frac{1}{2\pi\hbar}\exp[(\mathrm{i}/\hbar)(\kappa\lambda - \varepsilon\tau + 2\hbar\Delta(\tau, \lambda; \kappa, \varepsilon))]. \tag{4.1}$$

This form is chosen in analogy with (3.2) and (2.5) but it is general as long as Δ is a complex function. Without scattering potential, Δ is zero and $S = \mathbb{1}$.

For a central real potential, energy and angular momentum are conserved quantities. This means that

$$\langle \kappa, \varepsilon|S|\kappa', \varepsilon'\rangle \propto \delta(\varepsilon - \varepsilon') \qquad \langle \tau, \lambda|S|\tau', \lambda'\rangle \propto \delta(\lambda - \lambda'). \tag{4.2}$$

Calculation of these matrix elements from (4.1) tells us that Δ has to be independent of κ and τ to guarantee (4.2). The unitarity of the S matrix

$$\int\int \mathrm{d}\kappa\,\mathrm{d}\varepsilon\,\langle \tau, \lambda|S^+|\kappa, \varepsilon\rangle\langle \kappa, \varepsilon|S|\tau', \lambda'\rangle = \delta(\tau - \tau')\delta(\lambda - \lambda')$$

$$\int\int \mathrm{d}\tau\,\mathrm{d}\lambda\,\langle \kappa, \varepsilon|S|\tau, \lambda\rangle\langle \tau, \lambda|S^+|\kappa', \varepsilon'\rangle = \delta(\kappa - \kappa')\delta(\varepsilon - \varepsilon')$$

demands reality of Δ.

Since the original scattering Hamiltonian commutes with the shift operator A, we must demand that S and A commute. Using this fact and (3.9) we can write

$$\begin{aligned}\langle \kappa, \varepsilon | S | \tau, \lambda \rangle &= \langle \kappa, \varepsilon | ASA^{+} | \tau, \lambda \rangle \\ &= \exp(-i\lambda\pi/\hbar)\langle \kappa + \pi, -\varepsilon | S | -\tau, \lambda \rangle \\ &= \langle \kappa, -\varepsilon | S | -\tau, \lambda \rangle.\end{aligned}$$

The matrix elements are invariant for the change $(\varepsilon, \tau) \mapsto (-\varepsilon, -\tau)$. This is possible iff Δ is a function of $|\varepsilon|$. Finally

$$\langle \kappa, \varepsilon | S | \tau, \lambda \rangle = \frac{1}{2\pi\hbar} \exp\left[(i/\hbar)(\kappa\lambda - \varepsilon\tau + 2\hbar\delta_{\lambda}(|\varepsilon|))\right]. \tag{4.3}$$

The analogy with the classical result is complete. The exponent is identical with the classical generating function (2.5). The exact parametrisation (4.3) is defined for all real values of the angular momentum and the deflection angle is the derivative of $2\hbar\delta$ with respect to λ. Of course δ has to be calculated in a quantum way with the Schrödinger equation, but the interpretation of the result may be completely classical in the form (4.3).

Now, if we want to make a real scattering experiment we have the difficulty that neither angular momentum λ nor time τ are accessible. In fact, we prepare and detect some momentum p. But in our space $\mathcal{H}$, $\boldsymbol{P}$ do not constitute a complete set of commuting observables. We have to give the sheet n. This seems to be complicated but is of great advantage: $\langle p', n' | S | p, n \rangle$ is the probability amplitude to measure the momentum p' after the collisions if the state was prepared in the state $|p, n\rangle$ after an orbiting of $\frac{1}{2}(n' - n)$ turns around the potential.

A conventional detector is not sensitive to this number of turns, and by subtracting the initial beam, the probability amplitude of detection is

$$\begin{aligned}&\sum_{n'} \langle p', n' | S - \mathbb{1} | p, n \rangle \\ &\quad = \sum_{n'} \int\int\int\int d\kappa\, d\varepsilon\, d\tau\, d\lambda \langle p', n' | \kappa, \varepsilon \rangle \langle \kappa, \varepsilon | S - \mathbb{1} | \tau, \lambda \rangle \langle \tau, \lambda | p, n \rangle \\ &\quad = \frac{1}{2\pi\hbar m} \sum_{n'} \delta\left((-1)^{n} \frac{p^2}{2m} - (-1)^{n'} \frac{p'^2}{2m}\right) \\ &\qquad \times \int d\lambda \exp\left[-(i/\hbar)\lambda(\varphi - \varphi' + (n - n')\pi)\right]\{\exp\left[i2\delta_{\lambda}(p^2/2m)\right] - 1\}.\end{aligned}$$

Contributions to the sum arise for even differences $n' - n$. Again with the Poisson formula (A1) we obtain

$$\sum_{n'} \langle p', n' | S - \mathbb{1} | p, n \rangle = \frac{1}{2\pi m} \delta\left(\frac{p^2}{2m} - \frac{p'^2}{2m}\right) \sum_{l} \exp\left[il(\varphi' - \varphi)\right]\{\exp\left[i2\delta_{\hbar l}(p^2/2m)\right] - 1\}. \tag{4.4}$$

In this way we obtain the scattering amplitude in the usual form as given by Henneberger (1980) for the scattering in the plane. The kinematical factor in front is also traditional. As it should be, the result is independent of the initial arbitrary chosen sheet n.

In group theoretical language, the sum on n' is the projection onto the trivial representation of the ambiguity group. This projection picks up the integer values of the angular momentum $\lambda = \hbar l$, $l \in \mathbb{Z}$. Therefore, we lost important information but this weakness is not a disease of quantum mechanics. It is the result of a lack of imagination in the detection device.

In our opinion the usual limitation to integer values of l from the beginning is a root of the difficulties of the inverse problem. We need some interpolation devices which follows from more supplementary conditions imposed on the potential, usually locality.

5. Conclusion

The main result of this work is the need to introduce a sheeted phase space for the description of scattering. The sheets are related to the number of turns around the scatterer. In this way, the angular momentum takes all real values and the complete information on the collision is contained in the phaseshift, a derivable function of energy and angular momentum.

It seems that the use of an additional Aharonov–Bohm effect as a kind of interference plate would give access to other representations of the ambiguity group. In this way, the phase would be accessible (in principle) also for non-integer values of the angular momentum.

Appendix. Poisson formula for physicists

Starting from the usual formula (Berry 1980, Spiegel 1968)

$$\sum_n \int d\lambda\, F(\lambda) \exp(i2\pi n\lambda) = \sum_l F(l) \tag{A1}$$

and choosing $F(\lambda) = \exp(i2\pi x\lambda)$ we obtain

$$\sum_n \int d\lambda\, F(\lambda) \exp(i2\pi n\lambda) = \sum_n \int d\lambda\, \exp[i2\pi(n+x)\lambda]$$
$$= 2\pi \sum_n \delta(2\pi(n+x))$$

i.e.

$$\sum_n \delta(n+x) = \sum_n \exp(i2\pi nx). \tag{A2}$$

This is the translation in physicist notation of the result of Schwartz (1979) in distribution theory.

References

Amiet J P and Huguenin P 1980 *Helv. Phys. Acta* **53** 377

—— 1981 *Quantum mechanical representations of canonical transformations given by a generating function* to appear in *Helv. Phys. Acta* **55**

Berry M V 1980 *Eur. J. Phys.* **1** 240

Henneberger W C 1980 *Phys. Rev.* A **22** 1383
Hunziker W 1968 *Commun. Math. Phys.* **8** 282
Moshinsky M and Seligmann T H 1977 *Ann. Phys., NY* **114** 243
—— 1979 *Ann. Phys., NY* **120** 402
—— 1980 *Ann. Phys., NY* **127** 458
Narnhofer H and Thirring W 1981 *Phys. Rev.* A **23** 1688
Schwartz L 1979 *Méthodes Mathématiques pour les Sciences Physiques* (Paris: Hermann) p 217
Spiegel M R 1968 *Mathematical Handbook* (New York: Schaum) p 109
Van Vleck J H 1928 *Proc. Naut. Acad. Sci.* **14** 178
Zak J 1968 *Phys. Rev.* **168** 686

SEMI-CLASSICAL EXPANSION FOR THE SCATTERING BY A COMPLEX POTENTIAL

F. GUILLOD and P. HUGUENIN
Institut de Physique, Université de Neuchâtel, 1, rue A.L. Brequet, 2000 Neuchâtel, Switzerland

Received 21 December 1983

For the scattering by a complex potential the partial wave phase shifts are calculated to order $\hbar^2$ without using the method of complex trajectories. This shows how the imaginary part of the potential contributes to the deflection angle for different partial waves.

Let us consider a particle in a real central potential. By applying the usual WKB method to the Schrödinger equation one can find an approximation for the partial wave phase shift. However the singularity of the wave function at the classical turning point prevents one finding an asymptotic development in powers of $\hbar$ for the phase shift. This fact is clearly established for example by Rodberg and Thaler [1]. Generalising an idea of Miller and Good [2], Rosen and Yennie [3] have proposed a modified WKB approximation involving the solution of the free particle equation rather than the conventional exponential form. Thus they were able to add the correction of order $\hbar^2$ to the WKB phase shift. This correction improves greatly the numerical results and is useful to study the correspondence between the partial wave and impact parameter representations of the scattering amplitude [4].

In this letter we extend the Rosen and Yennie method to a complex central potential. Such a potential is used to describe the absorption of the incident beam due to inelastic scattering. In this case the radial Schrödinger equation reads

$$Eu = -(\hbar^2/2m)u'' + [V(r) - iW(r) + \hbar^2 l(l+1)/2mr^2]\,u\,, \qquad (1)$$

where the radial wave function u is defined by $\psi(r) = Y_{lm}(\theta,\varphi)u(r)/r$. The continuity equation

$$\nabla\cdot j = -(2W/\hbar)|\psi|^2 \qquad (2)$$

associated to the potential $V - iW$ fixes the sign of the imaginary part $-W$ in order to have an absorption of particles: it must be negative. This equation shows also that the classical limit $\hbar \to 0$ leads to the complete disappearance of a streamline which goes through a region where $W \neq 0$. This suggests a method of dealing with a potential whose imaginary part is proportional to $\hbar$. Therefore by setting $W = \hbar A$, where A does not depend on $\hbar$, we get a finite absorption even classically.

We now indicate the method of calculation used to find the phase shift to order $\hbar^2$ corresponding to the potenital $V - i\hbar A$. By making the Langer transformation [5]

$$r = (\hbar/p)\,e^{p\rho/\hbar}\,, \quad u(r) = e^{p\rho/2\hbar}\omega(\rho)\,, \qquad (3)$$

the Schrödinger equation (1) may be written as

$$\hbar^2\omega''(\rho) + e^{2p\rho/\hbar}[q^2(\rho) + i\hbar 2mA(\rho)]\,\omega(\rho) = 0\,, \qquad (4)$$

with

$$q^2(r) = 2m[E - \lambda^2/2mr^2 - V(r)]\,,$$

$$\lambda = \hbar(l+\tfrac{1}{2})\,, \quad p = \sqrt{2mE}\,.$$

We shall obtain an approximate solution of the differtial equation (4) by using the method of comparison equations [2], that is we assume

$$\omega(\rho) = \alpha(\rho)\omega_0(\sigma(\rho)/\hbar) + \beta(\rho)\omega_0'(\sigma(\rho)/\hbar)\,, \qquad (5)$$

where ω_0 satisfies the free particle equation

$$\omega_0''(\sigma/\hbar) + e^{2p\sigma/\hbar}q_0^2(\sigma)\omega_0(\sigma/\hbar) = 0\,, \qquad (6)$$

with $q_0 = q\,[V \equiv 0]$.

0.375-9601/84/$ 03.00

The problem then reduces to find the functions α, β and σ. We shall see that the coefficients α and β must depend on $\hbar$. Substituting the solution (5) into eq. (4) we obtain a linear combination between ω_0 and ω_0'. Equating the coefficients of ω_0 and ω_0' to zero we have

$$\hbar^2\alpha'' + i\hbar 2mA\, e^{2p\rho/\hbar}\alpha + [e^{2p\rho/\hbar}q^2 - e^{2p\sigma/\hbar}q_0^2(\sigma')^2]\alpha = 2\hbar\, e^{p\sigma/\hbar}q_0\sqrt{\sigma'}(e^{p\sigma/\hbar}q_0\sqrt{\sigma'}\beta)',$$

$$\hbar^2\beta'' + i\hbar 2mA\, e^{2p\rho/\hbar}\beta + [e^{2p\rho/\hbar}q^2 - e^{2p\sigma/\hbar}q_0^2(\sigma')^2]\beta = -2\hbar\sqrt{\sigma'}(\sqrt{\sigma'}\alpha)'. \quad (7)$$

To the lowest order in $\hbar$ the system (7) gives

$$e^{p\rho/\hbar}q(\rho) = e^{p\sigma/\hbar}q_0(\sigma)\sigma'. \quad (8)$$

By taking the boundary condition $p\sigma_t(\rho_t) = \hbar\log(\lambda/\hbar)$, where ρ_t and σ_t denote the classical turning points of q and q_0, the modified Hamilton–Jacobi equation (8) determines implicitly σ as a function of ρ. Conceptually it is important to remark that if the potential did not depend on $\hbar$, the turning point ρ_t would become complex. Such an approach, which has been well described by Thylwe and Fröman [6], leads to good numerical results (see for example Broglia et al. [7]) but the physical interpretation of a complex turning point is not clear in the classical limit $\hbar \to 0$. So we have obtained a second argument to require a potential whose imaginary part is proportional to $\hbar$.

With the condition (8) to system (7) reads

$$\hbar\alpha'' + i2mA\, e^{2p\rho/\hbar}\alpha = 2e^{p\sigma/\hbar}q_0\sqrt{\sigma'}(e^{p\sigma/\hbar}q_0\sqrt{\sigma'}\beta)',$$

$$\hbar\beta'' + i2mA\, e^{2p\rho/\hbar}\beta = -2\sqrt{\sigma'}(\sqrt{\sigma'}\alpha)'. \quad (9)$$

We solve the differential equations (9) asymptotically by expanding the unknowns α and β in powers of $\hbar$: $\alpha = \alpha_0 + \alpha_1\hbar + \ldots$ and $\beta = \beta_0 + \beta_1\hbar + \ldots$. By determining α_0, α_1 and β_0, β_1 we can find the phase shift to order $\hbar^2$ if the integration constants are chosen to have an incident plane wave plus a scattering term when $r \to \infty$. These long and tedious calculations lead to the result

$$\delta_l = \delta_l(\mathrm{WKB}) + i\hbar\int_{r_t}^{\infty} dr\, mA/q + \hbar^2\left[-\tfrac{1}{24}\int_{r_t}^{\infty} dr\,\frac{1}{rq}\left(\frac{4(E-V)-5rV'-r^2V''}{2(E-V)-rV'}\right)'\right.$$

$$\left. + \tfrac{1}{2}m^2\int_{r_t}^{\infty}\left(dr\,\frac{A^2}{q^3} - \frac{A_t^2}{[(r-r_t)(q_t^2)']^{3/2}}\right)\right] + O(\hbar^3), \quad (10)$$

with $A_t = A(r_t)$ and $(q_t^2)' = (q^2)'(r_t)$.

The first term of this development represents the usual WKB phase shift which is calculated from the real part of the potential only. It appears when we expand the function $\sigma(\rho)$ for large values of r. The second term arises from the coefficients α_0 and β_0. It is purely imaginary and thus it describes the absorption of particles. By using the formulation of the quantum mechanics on the phase space Amiet and Huguenin [8] have also found this attenuation factor [8]. The coefficients α_1 and β_1 lead to the terms which are proportional to $\hbar^2$. The former is the Rosen and Yennie correction [3] while the latter represents the contribution of the absorptive part of the potential to the real part of the phase shift.

Now we want to apply the above expression to two particular potentials. In the first example we choose

$$V = v/r^2 \quad (v \geq 0), \quad A = \alpha/r^2 \quad (\alpha \geq 0).$$

In this case the Rosen and Yennie correction vanishes and so the formula (10) gives

$$\delta_l = \tfrac{1}{2}\pi[\lambda - (\lambda^2 + 2mv)^{1/2} + i\hbar\, ma(\lambda^2 + 2mv)^{-1/2} - \tfrac{1}{2}\hbar^2 m^2a^2(\lambda^2 + 2mv)^{-3/2}] + O(\hbar^3). \quad (11)$$

For this potential we can solve exactly the Schrödinger equation to obtain

$$\delta_l = \tfrac{1}{2}\pi\,[\lambda - (\lambda^2 + 2mv - i\hbar 2ma)^{1/2}]. \quad (12)$$

The asymptotic expansion in powers of $\hbar$ of the exact result (12) coincides with the approximation (11). So this example justifies the introduction of the Langer transformation (3). Indeed if it was not carried out the approximation (11) would have a supplementary term coming from the Rosen and Yennie correction. Moreover the phase shift (11) would be a function of $l(l+1)$ rather than $(l+\frac{1}{2})^2$. Thus the expansion (11) would be coincide with the exact result to order $\hbar^2$.

The second example is more instructive and it is very useful in clarifying the following question: why does a purely imaginary potential produce an elastic cross section? In the classical limit $\hbar \to 0$ the absorptive part of the potential appears in the continuity equation (2) but it does not intervene in the equations of motion obtained with the hamiltonian of the Schrödinger equation (1). Thus classically the trajectory of a particle which moves in an imaginary potential remains always a straight line. Only an attenuation of the incident beam is expected. Therefore from this classical picture we do not see the diffraction effects in the quantum elastic cross section. To elucidate this situation we consider the scattering produced by the imaginary square well

$$V = 0, \quad A = a\theta(R - r) \quad a \geqslant 0.$$

Then the phase shift (10) gives

$$\delta_l = i\hbar(a/2E)(2mER^2 - \lambda^2)^{1/2} + \hbar^2(a^2/4E^2)(mER^2 - \lambda^2)(2mER^2 - \lambda^2)^{-1/2} + O(\hbar^3) \tag{13}$$

for $2mER^2 > \lambda^2$ and zero otherwise.

In a previous paper we have described the scattering in the plane by a real potential [9]. In this framework the derivative of the phase shift with respect to the angular momentum has been interpreted as the half of the deflection angle. This result can be generalised in three dimensions and for a complex potential in the following manner [7]

$$\Delta\varphi_l = 2\,\partial \operatorname{Re} \delta_l / \partial\lambda .$$

By evaluating this derivative for eq. (13) we find

$$\Delta\varphi_l = -\hbar^2(a^2\lambda/2E^2)(3mER^2 - \lambda^2) \times (2mER^2 - \lambda^2)^{-3/2} . \tag{14}$$

Therefore a particle which goes through an imaginary square well undergoes an attraction. We observe even an orbiting of the particle when its impact parameter approaches R. This is due to the discontinuity of the potential in R. Thus with this example we understand how two different partial waves can interfere: their trajectories are not straight lines as in classical mechanics. These interferences lead naturally to the elastic cross section. In addition we remark that the orbiting described above can be compared to the creep waves occurring in the scattering by a hard sphere [10].

With these two examples we have seen that it is relatively easy to calculate a correction to the usual semi-classical description of the scattering. In particular the contribution of the absorptive part of the potential (to order $\hbar^2$) for the phase shift can be very important, as was shown in the second example.

Let us recall that the calculations which lead to the final result (10) are based on an expansion in powers of $\hbar$ of the solution of the Schrödinger equation (1). In a next stage we would like to generalise this method to non-local potentials. By using the Weyl–Wigner formalism [8] we see that these potentials depend on the momentum. Thus a non-local potential can be considered as a function of $\hbar$, even if it is real. This new approach will have naturally to take this dependence on $\hbar$ into account. This point was not considered by Horiuchi [11] in his semi-classical study of non-local potentials.

In addition we should like to say that the method presented here can be also applied to optics and acoustics, for example. Indeed both domains are characterized by a wave equation which looks like a stationary Schrödinger equation.

We are indebted to J.-P. Amiet and J.-F. Germond for suggestions concerning the presentation of the manuscript.

References

[1] L.S. Rodberg and R.M. Thaler, Introduction to the quantum theory of scattering (Academic Press, New York, 1967).
[2] S.C. Miller and R.H. Good, Phys. Rev. 91 (1953) 174.
[3] M. Rosen and D.R. Yennie, J. Math. Phys. 5 (1964) 1505.
[4] S.J. Wallace, Phys. Rev. 8D (1973) 1846.
[5] R.E. Langer, Phys. Rev. 51 (1937) 669.
[6] K.E. Thylwe and N. Fröman, Ann. Phys. (NY) 150 (1983) 413.
[7] R.A. Broglia, S. Landowne, R.A. Malfliet, V. Rostokin and A. Winther, Phys. Rep. 11 (1974) 1.
[8] J.-P. Amiet and P. Huguenin, Mécaniques classique et quantique dans l'espace de phase (Université de Neuchâtel, Neuchâtel, 1981).
[9] F. Guillod and P. Huguenin, J. Phys. 15A (1982) 3705.
[10] B. Schrempp and F. Schrempp, Nucl. Phys. 163B (1980) 397.
[11] H. Horiuchi, Prog. Theor. Phys. 64 (1980) 184.

UNIVERSITE DE NEUCHATEL
LABORATOIRE DE BIOCHIMIE

FACULTE DES SCIENCES
PROFESSEUR E. STUTZ

ANALYSE DU GENE 16S SUPPLEMENTAIRE ET DES REGIONS ADJACENTES DANS LE GENOME CHLOROPLASTIQUE D'EUGLENA GRACILIS, Z

forme réduite
de la thèse

présentée à la Faculté des Sciences
de l'Université de Neuchâtel pour
obtenir le grade de docteur ès Sciences
option Biochimie et Biologie moléculaire

par

Etienne ROUX

- 1984 -

IMPRIMATUR POUR LA THÈSE

Analyse du gène 16S supplémentaire et des régions adjacentes dans le génome chloroplastique d'Euglena gracilis, Z

de M*onsieur Etienne Roux*

UNIVERSITÉ DE NEUCHATEL

FACULTÉ DES SCIENCES

La Faculté des sciences de l'Université de Neuchâtel, sur le rapport des membres du jury,

Messieurs E. Stutz, P. Schürmann, V. Nigon (Lyon) et J.D. Rochaix (Genève)

autorise l'impression de la présente thèse.

Neuchâtel, le *le 26 octobre 1984*

Le doyen:

H. Beck

H. Beck

PUBLICATIONS

- E. Roux, L. Graf and E. Stutz (1983)
  Nucleotide sequence of a 'truncated rRNA operon' of the Euglena gracilis chloroplast genome.
  Nucleic Acids Research 11:1957-1968

- E. Roux and E. Stutz (1985)
  The chloroplast genome of Euglena gracilis : the mosaic structure of a DNA segment linking the extra 16S rRNA gene with the rrn operon A.
  Current Genetics 9:221-227

Nucleotide sequence of a 'truncated rRNA operon' of the *Euglena gracilis* chloroplast genome

Etienne Roux, Lucia Graf+ and Erhard Stutz*

Laboratoire de Biochimie, Université de Neuchâtel, Ch. de Chantemerle 18, CH-2000 Neuchâtel, Switzerland

Received 18 February 1983; Revised and Accepted 11 March 1983

ABSTRACT

An extra 16S rRNA gene (s-16S rDNA) from the Euglena gracilis chloroplast genome and several hundred positions of its flanking regions have been sequenced. The structural part has 1486 positions and is to 98% homologous in its sequence with the 16S rRNA gene in functional chloroplast rRNA operons. Sequences of about 200 positions upstream and 15 positions downstream of the structural part of the s-16S rRNA gene region are highly homologous with corresponding parts in the functional operon. Neither tRNA genes (Ala, Ile) nor parts of the 23S and 5S rRNA genes are found within 557 positions after the 3' end of the s-16S rRNA gene, i.e., the 330 bp homology, observed in electron microscopic studies of heteroduplexes (4), between the s-16S rDNA downstream region and the 6.2 kb repeated segment containing the functional rRNA operon, must be due to a DNA stretch in the interoperon spacer. A structural model of the "truncated rRNA operon" is presented. Results from S-1 endonuclease analysis suggest that the s-16S rDNA region is probably not transcribed into stable s-16S rRNA.

INTRODUCTION

We have previously shown (1) that the circular chloroplast genome of the unicellular alga Euglena gracilis, Z-strain, contains, outside and about 3.1 kbp away from three contiguous and tandemly arranged rRNA operons (2), a single region in fragment EcoRI-B which strongly hybridizes with 16S rRNA but not with 23S rRNA. Further studies with the electron microscope (3,4) revealed important sequence homology between the 16S rRNA gene of a functional operon (f-16S rDNA) and the extra 16S rRNA gene (s-16S rDNA). Some of these results also suggested that sequence homology might include regions surrounding the structural part of the s-16S rRNA gene.

One of the three functional 16S rRNA genes (5), the corresponding 16S-23S rRNA intergenic spacer (6,7) and parts of its leader (7) were sequenced. It became evident that the E. gracilis chloroplast 16S rRNA gene is homologous to 72% with the respective E. coli gene and that the intergenic

spacer contains functional genes for $tRNA^{Ile}$ and $tRNA^{Ala}$ identical to e.g. the rrnD operon of E. coli (8). Furthermore, considerable sequence homology was found to exist between the 16S-23S intergenic spacer and parts of the leader region which happens to contain a cluster of pseudo-tRNA genes (7,9). In view of these results it became interesting to compare the sequences of the s-16S rRNA gene and its flanking regions with the corresponding regions in a functional operon and also to ask the question whether this "truncated operon" could and did yield a stable 16S rRNA in a proportionate amount.

In order to answer these questions we sequenced a stretch of 2474 positions, which includes the entire s-16S rRNA gene and several hundred positions of the flanking regions. We show in the following that the s-16S rRNA gene is identical with the f-16S rRNA gene to about 98%, one major difference being a deletion of nine base pairs. Large parts of the leader region are conserved including two pseudo-tRNA genes. Sequence homology stops soon after the 3' end of the s-16S rRNA gene, i.e., the region adjacent to the s-16S rRNA gene shows neither the functional tRNA genes nor the large subunit rRNA genes as found in the functional operons.

The nine base pair deletion in the s-16S rRNA gene allowed to test, by appropriate hybridization and S1-endonuclease protection analysis, whether the s-16S rRNA gene yields stable transcripts. According to the results given in this report, this gene region is not transcribed into stable 16S rRNA in an amount proportionate to its presence in the genome.

MATERIALS AND METHODS

The fragments BglII-H and G_1 had been previously mapped on the chloroplast genome (10). They were cloned into a modified pBR322 (11). Recombinant DNA was isolated and purified as recently described (5). DNA sequencing was according to Maxam and Gilbert (12) and as specified in (5). Enzymes were purchased from Boehringer-Mannheim and New England Biolabs and used following the instructions of the supplier; details are given in (5).

The 289 bp and 280 bp XbaI-HinfI fragments which were subsequently used in the S1-endonuclease protection analysis were cut from the BamHI-D fragment (13) and the BglII-H fragment (10), respectively. The fragments were purified and 5'-end labeled with [γ-^{32}P] ATP (3000 Ci/mmol,

Amersham). Strand separation and purification was done as published (5). 5'-end labeled single strands were hybridized as specified in the legend to Fig. 5. S1-endonuclease protection analysis was according to (14).

RESULTS

1. Sequencing strategy

The circular chloroplast genome of Euglena gracilis, Z, is very well characterized (2). A survey of all BglII sites in the rDNA region is given in Fig. 1, a, and aligned with it are the three rDNA operons and the extra 16S rRNA gene region (b). The sequenced s-16S rRNA gene region is shown in greater detail on line c. Under (d) we show the various restriction sites and fragments used in the sequencing work. The arrows represent portions of the 5'-end labeled fragments from which unambiguous sequences could be established.

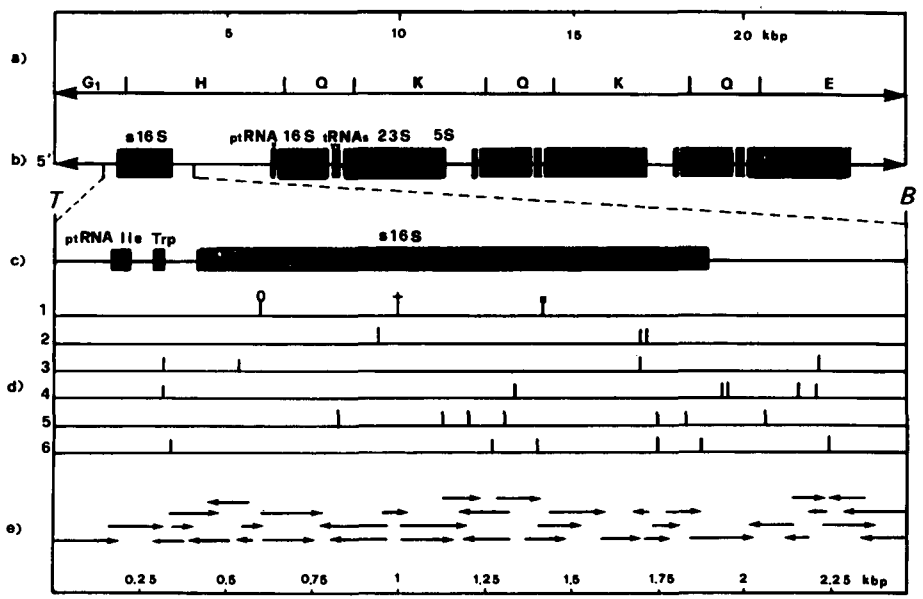

Fig. 1. Restriction endonuclease map and strategy used to sequence the s-16S rRNA gene region of the Euglena gracilis, Z, chloroplast DNA. a) BglII fragments, nomenclature see (10); b) map position of rRNA, tRNA and pseudo-tRNA genes according to published data (see text); c) s-16S rRNA gene region, T = TaqI, B = BamHI; d) restriction sites used for sequencing, 1 : BglII, HindIII, XbaI, 2 : HpaII, 3: HinfI, 4 : TaqI, 5 : HaeIII, 6 : RsaI; e) → RNA-like strand, ← coding strand.

TGGAAATGAC GAGTTTGATC CTTGCTCAGG GTGAACGCTG GCGGTATGCT TAACACATGC 60

AAGTTGAACG AAATTACTAG CAATAGTAAT TTAGTGGCGG ACGGGTGAGT AATATGTAAG 120

AATCTGCGCT TGGGTGAGGA ATAACAGATG GAAACGTTTG CTAATGCCTC ATAATTTACT 180

AGATCTATGT GAGTAGCTAG TTAAAGAGAA TTTCGCCTAG GCATGAGCTT GCATCTGATT 240

AGCTTGTTGG TGAGGTAAAG GCTTACCAAG GCGACGATCA GTAGCTGATT TGAGAGGATG 300

ATCAGCCACA CTGGGATTGA GAACGGAACA GACTTTTACG GAAGGCAGCA GTGAGGAATT 360

TTCCGCAATG GGCGCAAGCC TGACGGAGCA ATACCGCGTG AAGGAAGAAG GCCTTTGGGT 420

TGTAAACTTC TTTTCTCAAA GAAGAAGAAA TGACGGTATT TGAGGAATAA GCATCGGCTA 480

ATTCCGTGCC AGCAGCCGCG GTAATACGGG AGATGCGAGC GTTATCCGGA ATTATTGGGC 540

GTAAAGAGTT TGTAGGCGGT CAAGTGTGTT TAATGTTAAA AGTCAAAGCT TAACTTTGGA 600

AGGGCATTAA AAACTGCTAG ACTTGAGTAT GGTAGGGGTG AAGGGAATTT CCAGTGTAGC 660

GGTGAAATGC GTAGAGATTG GAAAGAACAC CAATGGCGAA GGCACTTTTC TAGGCCAATA 720

CTGACGCTGA GAAACGAAAG CTGAGGGAGC AAACAGGATT AGATACCCTG GTAGTCTTGG 780

CCGTAAACTA TGGATACTAA GTGGTGCTGA AAGTGCACTG CTGTAGTTAA CACGTTAAGT 840

ATCCCGCCTG GGGAGTACGC TTGCACAAGT GAAACTCAAA GGAATTGACG GGGGCCCGCA 900

CAAGCGGTGG AGCATGTGGT TTAATTCGAT GCAACACGAA GAACCTTACC AGGATTTGAC 960

AGGATCTAGG AGGAAGTTTG AAAGAACGCA GTACCTTCGG GTATCTAGAC ACAGGTGGTG 1020

CATGGCTGTC GTCAGCTCGT GTCGTGAGAT GTTGGGTTAA GTCCCGCAAC CCTTTTTTTT 1080

AATTAACGCT TGTCATTTAG AAATACTGCT GGTTATTACC AGAGGAAGGT GAGGACGACG 1140

TCAAGTCATC ATGCCCCTTA TATCCTGGGC TACACACGTG CTACAATGGT TAAGACAATA 1200

AGTTGCAATT TTGTGAAAAT GAGCTAATCT TAAAACTTAG CCTAAGTTCG GATTGTAGGC 1260

TGAAACTCGC CTACATGAAG CCGGAATCGC TAGTAATCGC CGGTCAGCTA TACGGCGGTG 1320

AATACGTTCT CGGGCCTTGT ACACACCGCC CGTCACACCA TGGAAGTTGG CTGTGCCCGA 1380

AGTTATTATC TTGCCTGAAA AGAGGGAAAT ACCTAAGGCC TGGCTGGTGA CTGGGGTGAA 1440

GTCGTAACAA GGTAGCCGTA CTGGAAGGTG TGGCTGGAAC AATTCGC 1477

Fig. 2. Nucleotide sequence of the s-16S rDNA. Only the RNA-like strand is given. Nucleotides differing from that of the f-16S rRNA gene are underlined [consult Table 1]. We mark the two possible 3' ends [Zablen et al. (15) versus Steege et al. (16), see text]. A 28 bp sequence in the 5' terminal part which is invertely repeated in the leader part [see Fig. 3] is marked by a wave line. An XbaI and HinfI site which are used to generate a 280 bp fragment [see Fig. 5] are boxed.

2. Comparison between the structural parts of the s-16S rRNA gene region and the f-16S rRNA gene

In Fig. 2 we show the nucleotide sequence of the entire s-16S rRNA gene which contains 1486 or 1487 positions depending on whether we take, respectively, as terminal RNase T1 oligonucleotide the one reported by Zablen et al. (15) or Steege et al. (16). The s-16S rRNA gene is five nucleotides shorter than the f-16S rRNA gene (5). Comparing the two sequences reveals a total of 21 mismatches, i.e., 98% sequence homology. We underlined in Fig. 2 those positions which differ from that in the f-16S rRNA gene and in Table 1 we qualify each mismatch. There are eight nucleotide changes (pos. 135, 336, 409, 423, 428, 1121, 1368, 1483) two insertions of one (pos. 771) and of three nucleotides (pos. 969 to 971), respectively, and a nine nucleotide deletion (pos. 1069). All these changes in the primary structure of the gene do not interfere with the secondary structure model of a potential 16S rRNA (17,18). Some of these base changes e.g. pos. 336 and 428 allow formation of an additional base pairing within a stem region. A minor secondary structure change could occur due to the nine bp deletion in the helix 29 which is part of the variable domain E

Table 1 : Sequence mismatches between the f-16S and the s-16S RNA gene of the E. gracilis, Z, chloroplast genome

f-16S (position)	s-16S (position)	Potential RNase T1 oligonucleotides (base change underlined)
C (135)	T (135)	
C (336)	T (336)	5'-ACUUUUACG [9 mer]
C (409)	A (409)	
A (423)	T (423)	5'-UAAACUUCUUUUCUCAAAG [19 mer]
C (428)	T (428)	
△ (770)*	G (771)	
△ (967)*	GGA (969-971)	
CGACGCCAA (1066-1074)	△ (1069)*	
G (1126)	A (1121)	5'-UUAUUACCAG [10 mer]
C (1373)	T (1368)	
C (1488)	T (1483)	

*Last identical position before mismatch.

[nomenclature according to Stiegler et al. (17)]. But as a whole we may consider the s-16S and f-16S rRNA genes to be structurally equivalent.

3. Analysis of the leader part

Electron microscopic analysis suggested that the sequence homology between the s-16S rRNA gene region and the f-16S rRNA gene includes also 150 bp preceeding the 5' end of the structural gene (4). Furthermore, Orozco et al. (7) sequenced parts of the leader of a f-16S rRNA gene and they found it to contain pseudo-tRNA genes or partial tRNA genes for isoleucin and alanine. R. Helling and collaborators have also sequenced the leader (pos. -1 to about -400) of a f-16S rRNA gene of Euglena gracilis, B-strain and they made the same observation (personal communication). It was therefore of interest to sequence the leader part of the s-16S rRNA gene. In Fig. 3 we show 415 positions upstream to the 5' end and align it with parts of the leader of a functional operon of the Z-strain (7). It contains a partial tRNA gene for alanine (codon change to tryptophane)

```
a)                          ACAAGAAA TAACTTAGCT TAATTCCTAG TGTAAATTTT
b) CTTATTTGCA AATTTAAAAG GCTTTTATCC TTTAGTAGTT AAGAAATCCA AGGATTTACT  -356

a) TCCGTATCTT AACGTGTGGA ACAATTTTTT TATTTTAATT AAAATACCGT ATAAATTTTA
b) GAAATTAAAC AATACTTATC ATTATGATGC GATATTTTTG TCAACTCAAA TATCCTTGAA  -296

a) AAAAATAAAA AAATCAAAAG GAAAATTTTT TATTTTTCAA AGATCACTAT TATCTTTTA.
b) TATCAAAATG TAAATGAGAT AAAAAACATG TTCAACTCTT TAGAAACGAC GTTAACTGCT  -236

a) ......A... ..C..... ..G..... .........G ..T....*** **********
b) TATTATGGAA TATCTTTGAT AAAGGTAGGG TCGTGGATTA AAGCCTTCGT TCAACTTGCA  -176

a) *******GTA T....C.... ...T..... T.......CC ......... .........
b) TGTGTTAAGC ATAGCTAAAT ATTGCTTTTC GTTAAAATTG TAAGCGCTAG GTCTCCAAAA  -116

a) .........A
b) CCTGATGTAG TAGGTTCGAA TCCTACAAAG CGCGCTTTTA GTGTACACAT TATAGTAAAT  - 56

a)                                        ..... T..... .....TGGAA
b) GTGCCCCTTG CTTGGTCACC AAGAGCGTGA AACGATTTGA CCAACTTTGA TGTTTTGGAA  +  5
```

Fig. 3. Nucleotide sequence of 415 positions preceeding the s-16S rDNA. Only the RNA-like strand is given (lines b) and aligned with a partially sequenced leader (lines a) of the f-16S rRNA gene as published (5,7). Points on line a indicate nucleotide identity with the sequence given on line b. Positions -21 to -105 on line a are left open. This segment has been sequenced in case of the B-strain and is to 98% identical with the sequence given in line b (R. Helling, authorized us to use his unpublished results). Stretches of pseudo-tRNA character (7,9) are underlined. The 20 bp insert is marked by asteriks. The inverted repeat of 28 bp corresponding to the sequence in the structural part of the 16S rRNA gene [see Fig. 2] is marked by a wave line. The first five positions of the 16S rRNA gene are framed.

and a pseudo-tRNA^{Ile} gene, but homology stops at position -236. We know that the DNA segment from pos. -1 to -106 of the s-16S rRNA gene leader is to 98% homologous with the corresponding leader part of the f-16S rRNA gene from the B-strain (R. Helling, personal communication). In particular the BstEII site (5'TTGGTCACCAA, pos. -44 to -34) is preserved where transcription might start according to a report of R. Hallick (NATO-FEBS Meeting, Porto-Portese, 1982). With a leader quite similar to that found in functional operons and an almost intact structural gene, the s-16S gene might serve as template for the RNA polymerase yielding 16S rRNA.

We mark on the s-16S leader (Fig. 3) an insert of 20 nucleotides which is not present in the f-16S leader. These 20 positions are part of a 28 bp sequence which occurs as an exact inverted repeat in the 5' terminal part of the s-16S rRNA gene (pos. 44 to 72).

4. Analysis of the sequence flanking the 3' end

In Fig. 4 we show 572 positions of the DNA segment flanking the 3' end of the s-16S rRNA gene. Sequence homology with the corresponding segment in the operon continues for 15 positions but within the next 557 positions we do not find any significant homology with the DNA segment following the f-16S rRNA gene, which contains the genes for tRNA^{Ile} and tRNA^{Ala} and the 5' terminal region of 23S rRNA (6,7). However, according to an interpretation of electron microscopic data of Koller and Delius (4) this segment should

```
TTTAGTTTTT TAACTGAATT TATTTATTAA TATTAACTCG ATTTTCGAGT AATTTTTATG   +60
ACTAACCGCT ATGTTAGTAT TTATGATGAT AATATGTGCA ATTAATTAAA CCAACAAATT  +120
GTCAAAAACT TCTCCTTTGA GTTTGAATTT TTCTGGCCAA AGCAGGATGC ATGGGAAGAA  +180
ATTAAAAAAT TTTTATATAG AAATCCGTGG ATTTCCGAGG ATATCGCTTT TAAACTTTAA  +240
ATGATATACG ATATTGTCGA GTGTTGGCAA AATGATTATG TTCTGCCAGA ATAGAACTGA  +300
TTAATCTGTC GAGGGAATCT TTTGGTTCTC TTTTAAAAGT CCGAAGAGTA CAAAATCAAG  +360
GTAAGCACTT TGACTTTTTC TCCTATGTTT TTGAATGGTT TTTTGCGCCG TCTTACGCGA  +420
AAAATAAAAC AACATGGCTA TGCGTTTTTT GTCGTTTCTG TTGATGGCAT AGCTACTGGC  +480
GTAAAAGGCT CCGTAAAAGG ATCTTTTTCT GTTGCTTCAC TTGACCCGAT GGTCATGGAA  +540
AATATAGAAA AATGTGCAAT ACTGCACAAT GA
```

Fig. 4. Nucleotide sequence of 572 positions following the 3'end (16) of the s-16S rDNA. The 15 positions homologous with the f-16S-23S intergenic spacer in a functional operon (6,7), the HaeIII site [see text], and the start of an open reading frame are underlined.

contain approximately 330 bp homologous with sequences flanking the 3' end of the 23S rRNA gene, i.e., it might contain a partial 5S rRNA sequence (consult Fig. 1). A computer search for 5S rRNA-like sequences within the 572 positions gave a negative result. According to previous restriction site analysis it seemed that sequence homology might extent at least up to the HaeIII site in the $tRNA^{Ile}$ gene of the intergenic spacer (1,7). Our sequencing data now reveal that a HaeIII site incidentally exists at the same distance from the 3' end yielding also a fragment of 225 bp, as was found in the intergenic spacer of the functional operon. However, the corresponding tRNA sequence is not present. We may add at this point that an open reading frame of unknown length starts at position 386. Whether this represents the start of a functional gene remains to be shown.

5. Search for s-16S rRNA

The nine bp deletion (pos. 1069) was used as a handle to test whether

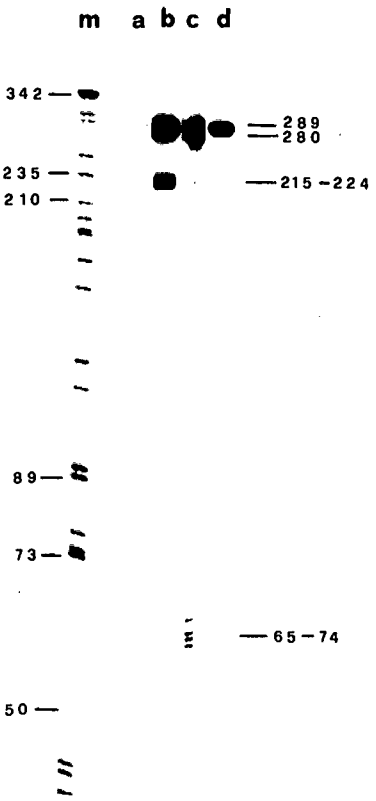

Fig. 5. Autoradiographs of the S-1 endonuclease protection analysis of DNA:DNA and DNA:RNA hybrids. 50 ng of 5' end labeled purified single strand DNA from the 289 bp fragment were hybridized with 25 ng of 5' end labeled purified single strand DNA from the 280 bp fragment in reciprocal experiments. Conditions : 3 h, 34°C, 40 mM PIPES, pH 6.4, 1 mM EDTA, 0.4 M NaCl, 80% formamide. 50 ng of the 5' end labeled purified coding strand from the 289 bp fragment were hybridized with 40 ng of total chloroplast RNA. Conditions : 3 h, 52°C, otherwise as mentioned above. S1-endonuclease digestion was in all cases for 30 min, 52°C, in 0.28 M NaCl, 0.05 M Na-acetate, pH 4.6, 4.5 mM $ZnSO_4$, 20 µg/ml carrier single strand DNA. Reaction volume in all cases 30 µl. Hybrids were analysed in sequencing gels (12). m) sizing marker, a) [289 bases, coding] alone, b) [289 bases, coding]X [280 bases, non coding], c) reciprocal version of (b), d) [289 bases, coding] X RNA. In panels b and c the top strong band is composed of the 289 and 280 bases ss DNA.

the "truncated rRNA operon" containing a leader and an intact 16S rRNA gene is transcribed yielding a proportionate amount of s-16S rRNA. To this end we cut from the f-16S rRNA and s-16S rRNA gene region a XbaI-HinfI DNA fragment of 289 and 280 bp, respectively, containing the nine bp insertion / deletion (see Table 1). These two DNA fragments were used in heterologous DNA:DNA and DNA:RNA hybridization experiments. The hybrids were analysed in S1-endonuclease protection experiments. In order to test the feasability of this approach we first constructed DNA heteroduplexes with purified 5' end labeled single strand DNA (ss DNA) from the 289 and 280 bp fragments. In Fig. 5 we show the electrophoretic analysis of the S1-endonuclease digestion products of the heteroduplexes. According to the position of the nine bp deletion in the XbaI-HinfI (280 bp) fragment (see Fig. 2) we should see in the autoradiograph ss DNA fragments of 216 and 65 bases in both cases, i.e., the combinations [289 bases, coding] X [280 bases, non-coding] and [289 bases, non-coding] X [280 bases, coding]. This is, however, under the given experimental conditions not the case. The first combination (panel b) yields a cluster of fragments in the range of 216-224 in addition to the intact fragments and the second combination yields a cluster of bands in the range of 65 to 74 (panel c) in addition to the intact fragments. The conclusion is that only the looping (longer) strand is cut while the shorter strand in the heteroduplexes remains essentially intact. In both cases the S1-endonuclease digestion of the heteroduplexes does not go to completion, yielding therefore a strong signal in the autoradiograph for the 289 and 280 bases ss DNA. On the other hand S1-endonuclease digestion is essentially complete if the 289 bases coding strand is used alone in the hybridisation experiment yielding a very faint signal (panel a) which is indicative for a pure ssDNA preparation.

Total chloroplast RNA was hybridized to the 5' end labeled 289 bases coding strand. The result of the S1-endonuclease protection analysis is shown in panel d. We see the expected strong signal in the range of 289 bases but we do not see any signal in the range of 215 to 224 bases. This strongly suggests that the s-16S rRNA is essentially absent in the chloroplast RNA preparation.

DISCUSSION

Comparison of the s-16S rDNA region with the f-16S rDNA region reveals

for the structural part of the gene essentially complete identity (98%). The most important change, namely the nine base pair deletion, would most likely not interfere with the functionality of the corresponding 16S rRNA since it does not involve any of the conserved regions (17). The only mutation of immediate functional impact might be the change in the so-called Shine-Dalgarno sequence (19) at pos. 1483 where a T(U) replaces a C. Note, however, that the chloroplast f-16S rRNA gene has already a modified Shine-Dalgarno sequence, i.e., instead of 5'-ACCUCC- as seen in E. coli DNA and, e.g., in the chloroplast DNA of maize (20) there is a 5'-AACUCC- in E. gracilis (5). Whether chloroplast mRNA is correspondingly adapted is not yet known.

Of considerable functional and evolutionary interest is a comparison of the leader parts. The first 164 positions proximal to the 5' end of the structural gene are almost identical with those from the f-16S rRNA gene of both the Z-strain and B-strain; homology continues for another 48 positions after an insert of 20 bp. Orozco et al. (7) and Myata et al. (9) have already discussed the fact that the leader region displays considerable homology with the intergenic spacer, including parts of the 3' end of the 16S rRNA gene and the $tRNA^{Ile}$ and $tRNA^{Ala}$ genes. The situation is very similar in our case, i.e., the same kind of pseudo-tRNA sequences are present in the leader part of the s-16S rRNA gene. Sequence homology between the "s-leader" and "f-leader" decreases to 40% and lower between position -235 and -415. This means that this part of the "s-leader" either has mutated during evolution more rapidly than the corresponding part in the "f-leader" or the postulated gene duplication event (9) never included that part of the s-leader.

Koller and Delius (4) have analysed DNA heteroduplexes formed between the s-16S and f-16S rDNA region. According to their electron microscopic measurements, sequence homology includes about 150 positions upstream of the structural part. Furthermore they observed a small loop (knob-like structure) upstream and in close proximity of the 5' end of the 16S rRNA gene. Our sequencing results of the leader part are in line with the electron microscopic analysis. The small loop seen in the heteroduplexes is most likely the result of a reannealing event between the 28 bases inverted repeats which are about 200 bases apart. The 20 bases insert in the leader is certainly too small to be seen in the electron microscope and therefore could not possibly be the reason for the knob-like structure (B. Koller, personal communication).

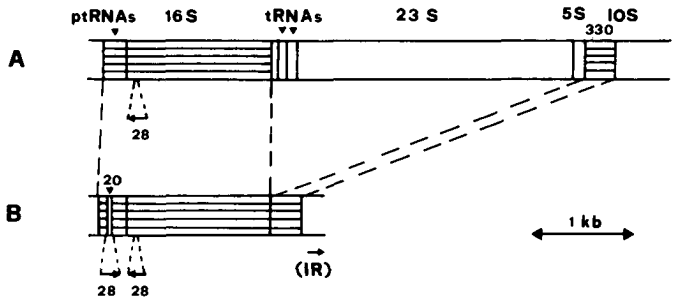

Fig. 6. Comparison of the anatomy of the functional rRNA operon [A] with the "truncated rRNA operon" [B]. Segments of high sequence homology are marked by boxes with horizontal bars; IOS : interoperon spacer; (IR) region of a small inverted repeat described in (4).

According to electron microscopic analysis a stretch of about 330 nucleotides downstream of the s-16S rRNA gene interacts with a region in the functional operon adjacent to the 3' end of the 23S rRNA gene possibly including parts of a modified 5S rRNA gene (4). We did not find a 5S rRNA-like sequence within the 330 bp adjacent and downstream of the s-16S rRNA gene. Therefore, the observed interaction must be due to a matching sequence located after the 5S rRNA gene of one operon and before the leader part of the next operon, i.e., within the interoperon spacer (2) as shown in Fig. 6. The average A+T content of this 330 bp stretch is about 70% (Fig. 2). Accordingly, the s-16S rRNA gene region would contain a leader part and a 16S rRNA gene very similar to the functional operon, including 15 positions of the intergenic spacer and about 330 bp of the interoperon spacer as schematically drawn in Fig. 6. It is noteworthy that s-16S rDNA also occurs in the chloroplast genome of the bacillaris strain of Euglena gracilis (21).

s-16S rRNA was not detectable in our hybridisation experiments and none of the potential T1-oligonucleotides (see Table 1) was listed by Zablen et al. (15). This could mean that the s-16S rDNA is not transcribed at all or that it is transcribed at normal rate like the normal rDNA regions but the steady state concentration of the s-16S rRNA remains below detectability due to rapid degradation of the transcription product after synthesis.

ACKNOWLEDGEMENTS

We are grateful to R.B. Helling (Ann Arbor) for providing unpublished sequencing data, M. Fasnacht, B. Jenni and B. Schlunegger for providing

the clones, P.E. Montandon for suggesting the experiments concerning the rDNA transcription and Ch. Bachmann for secretarial help. The computer programs were obtained from R. Staden, Cambridge. This research is supported by Fonds national suisse de la Recherche scientifique (3.183.82 to E.S.). This work is part of a Ph.D. thesis (E.R.).

+Present address: Friedrich Miescher-Institute, P.O. Box 2543, CH-4002 Basel, Switzerland

*To whom correspondence should be addressed

REFERENCES

1. Jenni, B. and Stutz, E. (1979). FEBS Lett. 102, 95-99.
2. Hallick, R.B. The Biology of Euglena, vol. IV, Buetow, D.E., ed., Academic Press, New York, in press.
3. Koller, B. and Delius, H. (1982). FEBS Lett. 139, 86-92.
4. Koller, B. and Delius, H. (1982). FEBS Lett. 140, 198-202.
5. Graf, L., Roux, E., Stutz, E. and Kössel, H. (1982). Nucleic Acids Res. 10, 6369-6381.
6. Graf, L., Kössel, H. and Stutz, E. (1980). Nature 286, 908-910.
7. Orozco, E.M. jr., Rushlow, K.E., Dodd, J.R. and Hallick, R.B. (1980). J. Biol. Chem. 255, 10997-11003.
8. Young, R.A., Maklis, R. and Steitz, J.A. (1979). J. Biol. Chem. 254, 3264-3271.
9. Miyata, T., Kikuno, R. and Ohshima, Y. (1982). Nucleic Acids Res. 10, 1771-1780.
10. Jenni, B., Fasnacht, M. and Stutz, E. (1981). FEBS Lett. 125, 175-179.
11. Schlunegger, B., Fasnacht, M., Stutz, E., Koller, B. and Delius, H. (1983). Biochim. Biophys. Acta 739, 114-121.
12. Maxam, A.M. and Gilbert, H. (1980). Methods in Enzymology, vol. 65, pp. 499-560, Grossman, L. and Moldave, K., eds, Academic Press, New York.
13. Gray, P.W. and Hallick, R.B. (1978). Biochemistry 17, 284-290.
14. Favaloro, J., Treisman, R. and Kamen, R. (1980). Methods in Enzymology 65, pp. 718-749, Grossman, L. and Moldave, K., eds, Academic Press, New York.
15. Zablen, L.B., Kissil, M.S., Woese, C.R. and Buetow, D.E. (1975). Proc. Natl. Acad. Sci. USA 72, 2418-2422.
16. Steege, D.A., Graves, M.C. and Spremulli, L.L. (1982). J. Biol. Chem. 257, 10430-10439.
17. Stiegler, P., Carbon, P., Ebel, J.P., Ehresmann, C. (1981). Eur. J. Biochem. 120, 487-495.
18. Zwieb, Ch., Glotz, C. and Brimacombe, R. (1981). Nucleic Acids Res. 9, 3621-3640.
19. Shine, J. and Dalgarno, L. (1974). Proc. Natl. Acad. Sci. USA 71, 1342-1346.
20. Schwarz, Zs. and Kössel, H. (1980). Nature 283, 739-742.
21. Koller, B. and Delius, H. (1982). Mol. Gen. Genet. 188, 305-308.

Current Genetics (1985) 9:221–227

Current Genetics

The chloroplast genome of *Euglena gracilis:* the mosaic structure of a DNA segment linking the extra 16S rRNA gene with the *rrn* operon A

Etienne Roux and Erhard Stutz

Laboratoire de Biochimie, Université de Neuchâtel, Ch. de Chantemerle 18, CH-2000 Neuchâtel, Switzerland

Summary. We have completed the analysis of a DNA segment of the chloroplast genome of *Euglena gracilis* Klebs, Z-strain, which links the 3′ end of the extra 16S rRNA gene with the 5′ end of the 16S rRNA gene of the *rrn* operon A. This region is a mosaic of several structural elements and contains an intact *rrn* interoperon spacer of 1,080 bp, an extra 5S rRNA gene, an open reading frame for 406 codons (ORF 406) which is flanked by short inverted repeats and a short direct repeat originating from the *rrn* interoperon spacer. It seems that a once complete *rrn* operon underwent in the past an insertion/deletion event leaving intact the 16S and 5S rRNA but totally excising the 16S-23S intergenic spacer and the 23S rRNA gene. Instead a protein coding gene of yet unknown function was inserted along with other structural elements.

Key words: Chloroplast DNA – *Euglena gracilis* – *rrn* operons – DNA deletion/insertion

Introduction

Several years ago, Jenni and Stutz 1979, reported for the first time that the circular chloroplast genome of *Euglena gracilis* Klebs, Z-strain, contains in addition to three tandemly arranged *rrn* operons [5′-16S-*trn*A-*trn*I-23S-5S-3′] an extra 16S rRNA gene (s16S) about 3.1 kbp upstream of the 5′ end of the next 16S rRNA gene (*rrn* operon A). We sequenced both the 16S rRNA gene of the *rrn* operon A (Graf et al. 1982) and the s16S rRNA gene (Roux et al. 1983) and found a very high sequence homology of 98%, suggesting that this s16S rRNA gene could yield functional 16S rRNA. More recently the s16S rRNA gene was found in other strains of *Euglena gracilis*, e.g., *bacillaris* and Z-S strain (Koller et al. 1984) which contain three and one *rrn* operon, respectively. It was also found in the strain American Type Culture Collection ATCC 10,616 which contains five *rrn* operons (Koller and Delius 1982a; Flamant et al. 1984). In this particular case there are two s16S genes located upstream of the first and third *rrn* operon, respectively. Also an X-ray induced mutant (Y3 BUD) of the *bacillaris* wild type which has lost the *rrn* operon A has retained the s16S rRNA gene in front of the first *rrn* operon (Ravel-Chapuis et al. 1984). From these results, we may conclude that the number of *rrn* operons per circular chloroplast genome can vary without impairing normal growth, however, a s16S rRNA gene is always present and located upstream of the first complete *rrn* operon. This strongly suggests that this DNA stretch or parts of it carries genetic information vital for the *Euglena gracilis* chloroplast.

Very recently, Koller et al. (1984) have studied in the electron microscope homo- and heteroduplexes formed between chloroplast DNAs from the *bacillaris* and Z-S strain. This study included also the DNA region between the s16S and 16S rRNA genes. From these and similar studies with the Z-strain (Koller and Delius 1982b) it became evident that this DNA segment is composed of several structural elements like, e.g., short direct and indirect repeats and that the arrangement of these elements in the various strains follows a somewhat similar pattern. Parts of this segment have recently been sequenced both in the *bacillaris* strain (El-Gewely et al. 1984) and in the Z-strain (Roux et al. 1983). Based on these sequencing data and the electron microscopic results it was suggested that the s16S rRNA gene is a relic of a once complete *rrn* operon which was "truncated" during a DNA insertion/deletion event in a distant past.

We report here the nucleotide sequence of the entire DNA segment between the s16S and 16S rRNA genes of

Offprint requests to: E. Stutz

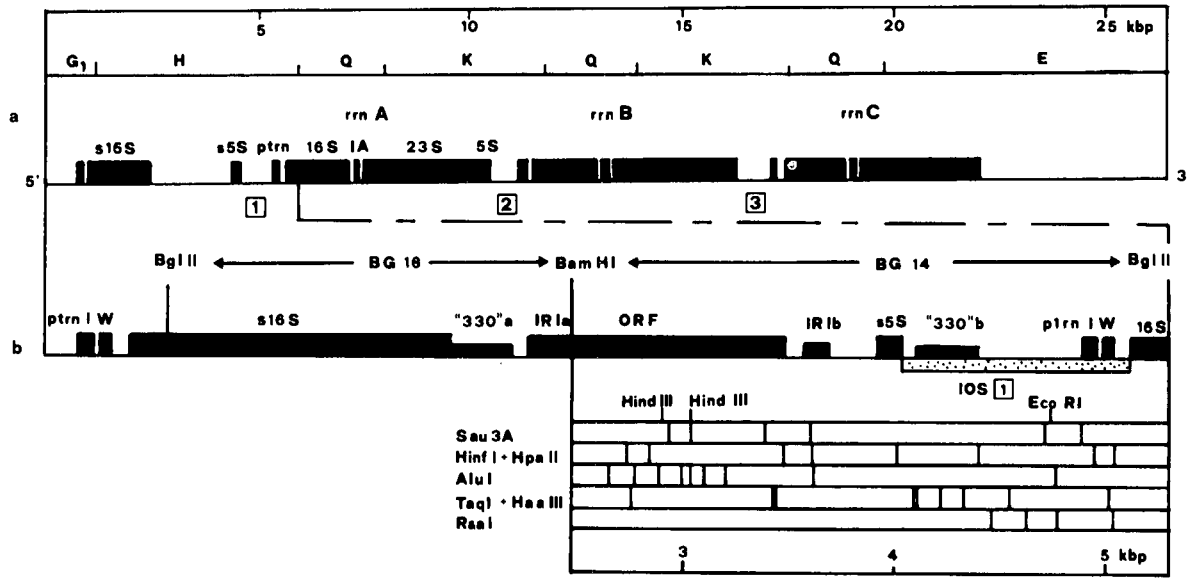

Fig. 1 a–c. Map position and strategy of sequencing. a BglII site restriction map (Jenni et al. 1981) of the rDNA region with the extra 16S rRNA gene and the *rrn* operons A, B, C (Hallick 1984). b Structural elements of the previously sequenced DNA stretch (Roux et al. 1983) and the fragment BG14 analysed in this report. c Restriction fragments used for sequencing according to Sanger et al. (1980). The interoperon spacers (IOS) are ordered 1, 2, 3 and defined in the text. The structural element "330", IR1a,b and ORF are defined in the text. s16S and s5S are the structural parts of 16S and 5S rRNA genes of the "truncated" *rrn* operon upstream of interoperon spacer 1, ptrn are the pseudo-tRNA genes for Ile and Trp previously described (Roux et al. 1983), I, W are the *trn*I and *trn*A genes of the intergenic spacer (Graf et al. 1980)

the Z-strain. This allows to precisely define the structural elements observed in the electron microscope and to compare on a nucleotide level the interoperon spacers of the Z- and *bacillaris* strain. These sequencing studies also reveal a major open reading frame which is co-transcribed with the s16S rRNA gene as will be shown elsewhere (Roux, Koller, Montandon and Stutz, to be published).

Materials and methods

Euglena gracilis, Klebs, Z-strain was purchased some time ago from the Culture Collection of Algae at Indiana University, strain number 753 (Starr 1964). The chloroplast genome of this strain and in particular the rDNA region has been described in great detail (Hallick 1984).

Enzymes were purchased from Boehringer-Mannheim and used following the instructions of the supplier. [α-^{32}P]ATP 400 Ci/mmole was from Radiochemical Center, Amersham.

The chloroplast DNA fragment BglII-H was cloned into the BglII site of a modified pBR322 (Schlunegger et al. 1983).

As starting material for DNA sequencing we used the BamHI-BglII DNA fragment BG14 (Jenni and Stutz 1979), which was obtained from the cloned fragment BglII-H (4.7 kbp). Subfragments of BG14 were routinely filled with the Klenow fragment of DNA polymerase (Wartell and Reznikoff 1980) and cloned into the HincII site of phage M13 mp9 (Messing et al. 1980; Messing and Vieira 1982) with ligation conditions as reported by Tait et al. (1980). Transformation of *E. coli* JM103 was according to Cohen et al. (1972), however, competent cells were prepared in 0.02 M Tris-HCl, pH 7.2, 0.1 M $CaCl_2$, 0,001 M NaCl.

DNA sequencing was according to Sanger et al. (1980).

Results

Mapping and strategy of sequencing

In Fig. 1 (a) we show the BglII fragments of a DNA segment of the circular chloroplast genome as mapped previously (Jenni et al. 1981). Line (b) gives the position of all the structural elements as defined and discussed in this report and under (c) we show the restriction fragments used in nucleotide sequencing experiments.

Nucleotide sequence and major structural elements

In a previous paper (Roux et al. 1983) we reported the nucleotide sequence of a DNA segment which started within the fragment BglII-G1 and ended with the BamHI site in BglII-H (see Fig. 1). In order to relate those sequencing results with the new data given here we display again in Fig. 2 the 3′ end of the s16S rRNA gene (pos. 1902) and the adjacent part up to position 2477 (see BamHI site). This stretch contains one of the "330" elements and one of the IR1 elements, seen by Koller and Delius (1982) in the electron microscope. With the complete sequence at hand we can now define both the "330" and the IR1 elements. The "330"a (293 nucleotides) and the "330"b (303 nucleotides) are homologous to

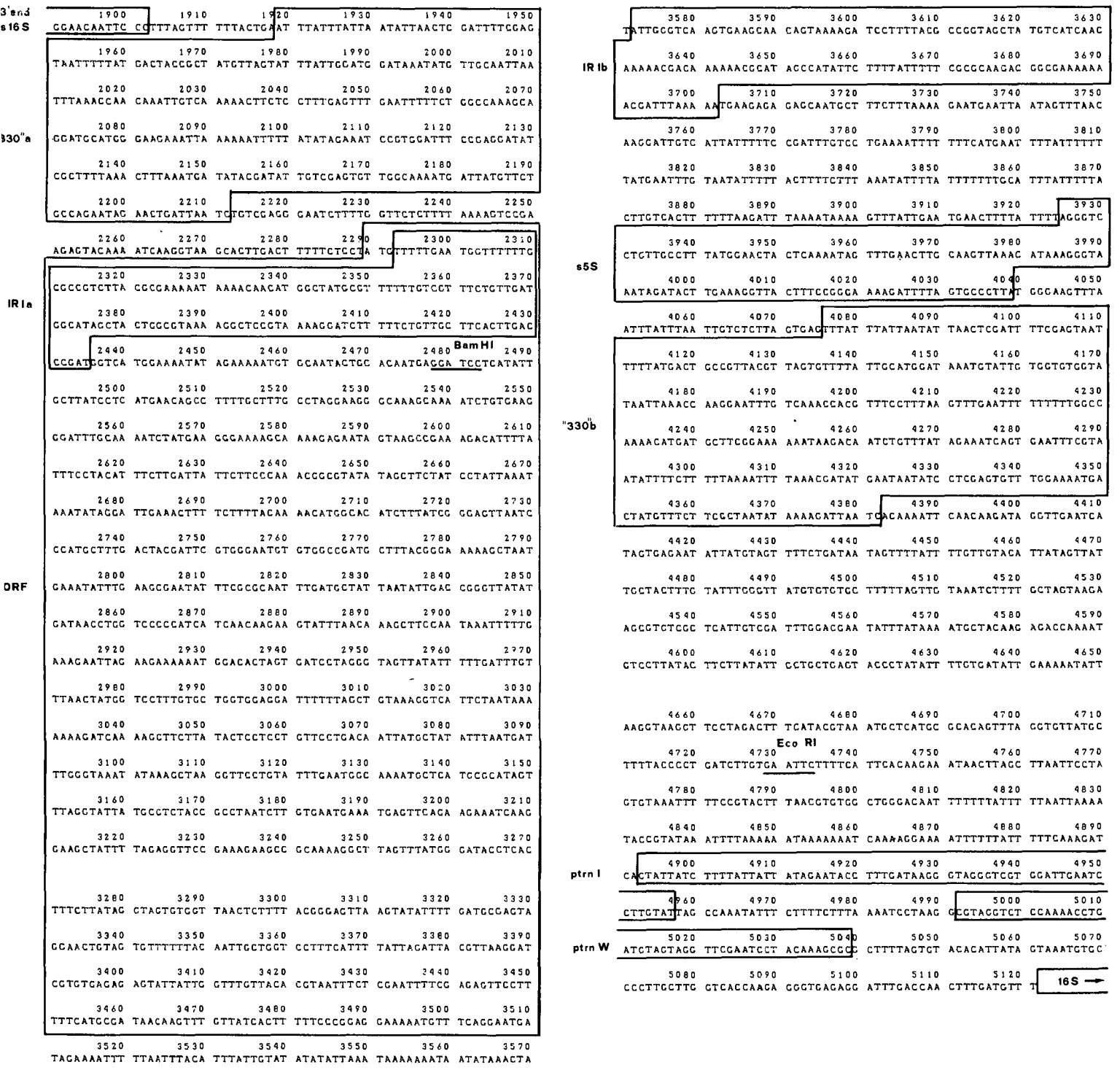

Fig. 2. Nucleotide sequence of a DNA segment linking the 3′ end of the s16S rRNA gene with the 5′ end of the 16S rRNA of *rrn* operon A. Only the DNA strand corresponding to the rRNA strand is shown. Major structural elements are boxed and important restriction sites underlined

about 75%, they are relatively rich in A+T (around 70%) and represent the only major direct repeats in the analyzed segment.

The two elements IR1a (143 nucleotides) and IR1b (131 nucleotides) match to 84%. They have an A+T content of about 60% and no other indirect repeats of this size are found in the analyzed segment. Interesting enough IR1a is part of an open reading frame sitting right at the 5′ end, while IR1b is 61 positions downstream of the protein coding region.

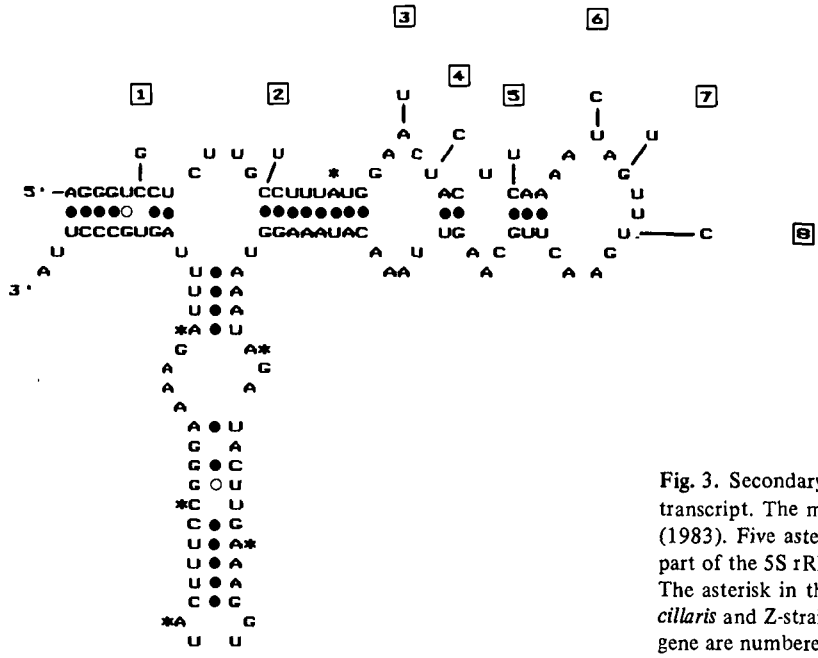

Fig. 3. Secondary structure model of a hypothetical s5S rDNA transcript. The model is constructed according to Karabin et al. (1983). Five asterisks denote the polymorphism found in the 3′ part of the 5S rRNA gene of *rrn* operon A, B and C, respectively. The asterisk in the 5′ part marks a base change between the *bacillaris* and Z-strain. Changes in the 5′ part found in the s5S RNA gene are numbered 1 to 8

MFLNGFLRRLTRKIKQHGYAFFVVSVDGIATGVKGSVKGSFSVASLDFMVMENIEKCAIL
HNEDPHIAYPHEQPFALPRKGKAKSVKGFAKSMKGKAKENSKPKDILFPTFLDYSSQTAY
IASILLNKYRIETFLLQNMAHLYRELIPCFDYDSWECVADALREKANEIFEANISRNLML
LILTGLYDNLVPHHQDEVFNKASNKFLKELEEKMDTSDPRVVIFLICLTMVLCAGGGFFS
CKRHSNKKRSKASYTPPVPDNYAIFNDLGKYKAKVPVFEWQNAHAHSLGIMPLPPNLVNE
MSSEEIKEAILEVPKEAAKGLVYGIPHFLIGSVVNSFTGVKYILMRVGTVVFFTIAGPFI
LLDYVKDRVREYYWFVTRNFSNFREFLFHAITSLLSLFPGGKMFQE

Fig. 4. Aminoacid composition of the translation product of ORF 406 as deduced from the nucleotide sequence, the deduced molecular weight is 46,100

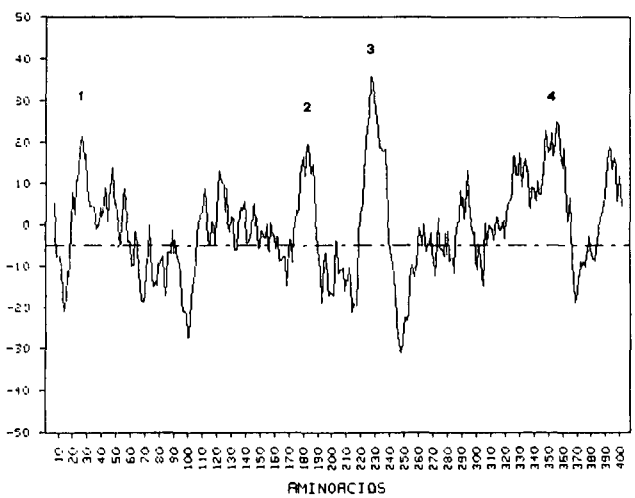

Fig. 5. Hydropathy plot of the 46,100 d protein of ORF 406. Each point on the profile corresponds to the sum of the hydropathy values of 11 adjacent aminoacids calculated according to Kyte and Doolittle (1982). Four hydrophobic region of 20 or more residues are marked 1 to 4. This computer analysis was kindly done by J. M. Erickson, University of Geneva

A complete 5S rRNA gene was retrieved, starting at position 3925. This was anticipated for the Z-strain according to results based on electron microscopic observations from Koller and Delius (1982b). An identical situation occurs also in the *bascillaris* and Z-S strain (Koller et al. 1984). We show in Fig. 3 the secondary structure model of a potential transcript and compare it with the sequence of Z-strain chloroplast 5S rRNA genes known to slightly diverge among the three *rrn* operons (Karabin et al. 1983). It is noteworthy that the s5S rRNA gene differs in eight positions all situated in the 5′ part, while sequence divergences of the 5S rRNA genes of *rrn* operons A, B, C are all located in the 3′ part. It seems that the s5S rRNA is not transcribed, since no corresponding rRNA product was identified (Karabin et al. 1983).

As structural interoperon spacer we define the DNA stretch between the 3′ end of the 5S rRNA gene and the 5′ end of the 16S rRNA gene of the next *rrn* operon. The functional *rrn* operon starts and ends somewhere within this region. According to a suggestion of EL-Gewely et al. (1984), the sequences 5′-TGGGACA (pos. 4782) and 5′-TAAAAT- (pos. 4826) may be promoter sites and the short indirect repeat 5′-ACTCGA- (pos. 4093) which is integral part of the "330" element may act as transcription terminator. These sequences are preserved in all interoperon spacers analysed so far. It is known for some time that two pseudo-tRNA genes (Ala, Trp) are proximate to the 5′ end of the 16S rRNA gene. We see them also in interoperon spacer 1 of the Z-strain (pos. 4906 and 4996).

A major open reading frame (ORF 406) starts at position 2290 (ATG) and terminates at position 3510 (TGA).

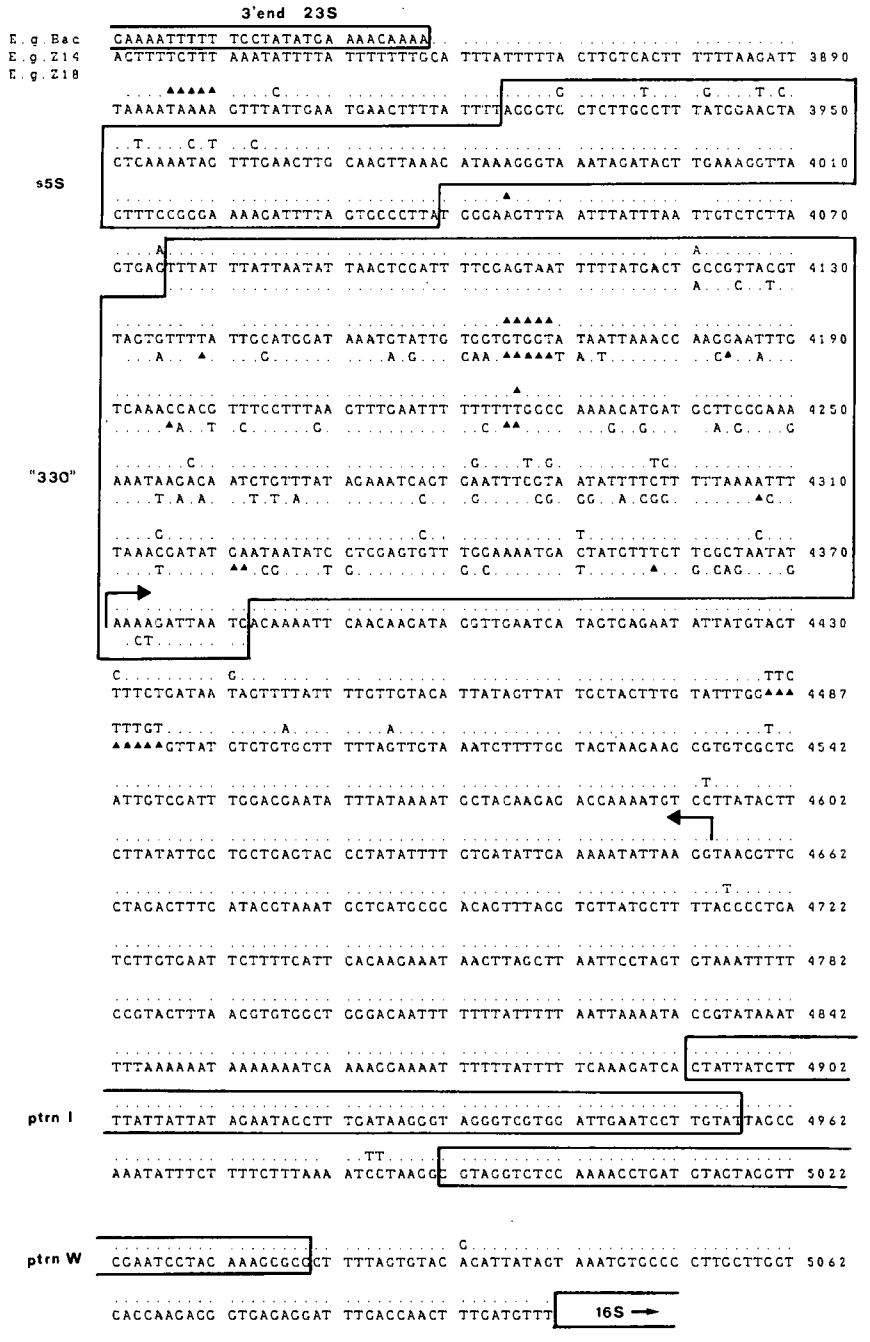

Fig. 6. Sequence comparison of interoperon spacer 1 of the Z- and *bacillaris* strain. Major structural elements are boxed. Within the "330" box we add the sequence of the "330"a element of the BG18 fragment of the Z-strain. Bent arrows mark the deletion in interoperon spacer 2 of the *bacillaris* strain (El-Gewely et al. 1984). We add the 3′ part of the 23S rRNA gene of the bacillaris strain to show that in the Z-strain counterpart there is no 23S rRNA gene. Note, however, that upstream of the s5S rRNA gene of the *bacillaris* strain exists an inverted repeat of the "330" element (consult Fig. 7)

We give in Fig. 4 the deduced aminoacid sequence and in Fig. 5 the corresponding hydropathy plot. We recognize four hydrophobic domains (1 to 4) comprising at least 20 aminoacids required, e.g., to traverse a thylakoid membrane. The protein is not identical or related to any of the sequenced chloroplast proteins, but as will be shown elsewhere (Roux et al. in preparation) the gene is actively transcribed.

Discussion

Interoperon spacer 1 and the "330" element

El-Gewely et al. (1984) sequenced the *rrn* interoperon spacers 2 and 3 of the *Euglena gracilis bacillaris* strain including large parts of the interoperon spacer 1 and parts of the s5S rRNA gene. We compare in Fig. 6 the corres-

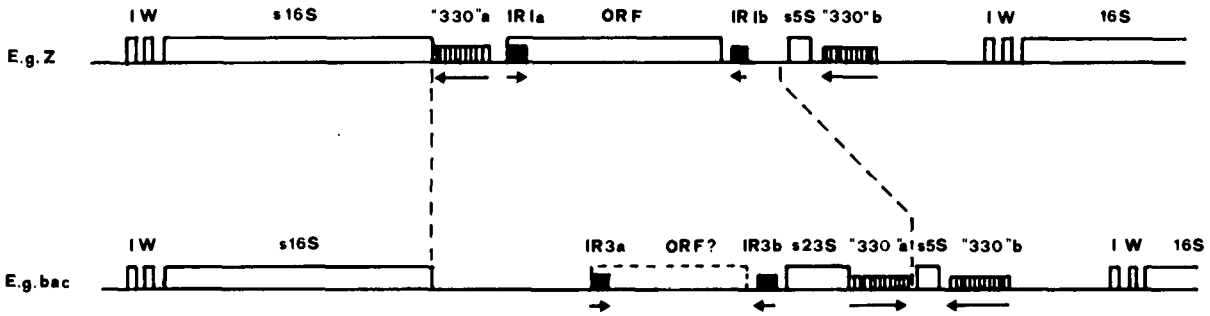

Fig. 7. Comparison of the mosaic structure of the DNA segment linking the s16S rRNA genes of the Z- and *bacillaris* strain. The structural elements are drawn in scale based on results from Koller et al. (1984) and El-Gewely et al. (1984) (*bacillaris*) and Roux et al. (1983) and this report (Z-strain). I, W = pseudogenes for Ile and Trp. Arrows indicate the relative orientation of repeats. The segment up-stream of the s5S rRNA gene including the s16S gene and its leader part of the *bacillaris* strain have not been sequenced

ponding region of the Z- and *bacillaris* strain and find a sequence homology of 97%. A most conspicuous difference is a five bases deletion (pos. 4165, Z-strain). The two strains may have separated about 15 x 10^6 years ago (see El-Gewely et al. 1984, for details of strain origin). Under this assumption it is surprising that the interoperon spacer 1, linking a "truncated" with a functional *rrn* operon is so well conserved, if on the other hand interoperon spacer 2 is 293 nucleotides shorter than interoperon spacer 3, which both link functional *rrn* operons (*bacillaris* strain). In the Z-strain the three interoperon spacers are of identical length and composition according to restriction site mapping (Hallick 1984), electron microscopic data (Koller and Delius 1982) and this and previous sequencing results (Graf et al. 1982).

A major DNA segment of the interoperon spacer ("330" element) is repeated proximate to the 3′ end of the s16S rRNA gene of the Z-strain. Probably the same segment is also repeated and inversely inserted upstream of the s5S of the *bacillaris* and Z-S strain according to electron microscopic observations (Koller et al. 1984). In Fig. 6 we align the two "330" elements of the Z-strain with the counterpart of the *bacillaris* strain. We calculated the degree of sequence divergence of the three "330" elements. The results are as follows: "330"a (Z-) : "330"b (Z-) = 0.23; "330"b (*bacillaris*) : "330"b (Z-) = 0.06; "330"a (Z-) : "330"b (*bacillaris*) = 0.20. According to these results the "330"a element drifted much more that the "330"b elements inside of the interoperon spacer 1 of both the Z- and *bacillaris* strain. It is noteworthy that the "330"a element of the Z-strain lacks the same five nucleotides as the "330"b element of the interoperon spacer 1 of the *bacillaris* strain. Since the "330"a element of the *bacillaris* strain has not been sequenced it is too early to establish a more elaborate pedigree of the "330" elements. We may nevertheless ask the question, whether the "330" elements qualify for some sort of mobile genetic element which may enhance DNA rearrangements like e.g. deletions and insertions (Starlinger 1977). A structural hallmark of IS elements and transposons are terminal repeats, what is not seen in our case. It will be of interest to analyse on a nucleotide level "330" elements from various Euglena strains and to search for such elements elsewhere on the chloroplast genomes.

Relics of chloroplast rrn operons and the ORF 406

Based on electron microscopic data (Koller et al. 1984) and nucleotide sequencing studies (Roux et al. 1983) it was postulated that the s16S rRNA gene is a relic of a once intact *rrn* operon. The present results give further support for this assumption in particular the findings that the interoperon spacer 1 is highly conserved and that a s5S rRNA gene is retained. It seems therefore highly plausible that due to a deletion/insertion event in the evolutionary past a DNA piece of about 3 kb was excised (the 16S-23S intergenic spacer with the *trn*I and *trn*A and the 23S rRNA gene) and replaced by an insert of about 2 kb consisting mainly of a directly repeated "330" element and a ORF flanked by short inverted repeats (IR1).

A somewhat similar situation is seen in the *bacillaris* strain. Koller et al. (1984) also observed the s16S and s5S rRNA genes separated by an insert which contains a "330" element, the short inverted repeats and a slightly shortened version of the ORF region. In addition they observed a short piece (300 to 350 nucleotides) of the 3′ part of the 23S rRNA gene. In Fig. 7 we compare the anatomical situation of the Z-strain with that of the *bacillaris* strain.

The question arises when in the evolutionary past such a major DNA rearrangement (s) occured, before or after separation of the two strains. An answer may be obtained by further sequencing the various structural elements upstream of the s5S rRNA gene of the *bacillaris* strain, notably the "330" elements, the inverted re-

peats and the segments in between. We favour right now the assumption that the major deletion/insertion event happened before strain separation what could explain the apparent identity of the ORF region and its flanking inverted repeats in both strains. The tandemly arranged *rrn* operons are prone to unequal-crossing events which easily lead to the observed variation in the number of *rrn* operons in the various Euglena chloroplast genomes. All the more it is surprising that the "truncated" *rrn* operon has survived during evolution in the various strains.

Acknowledgements. We are grateful to J. M. Erickson, University of Geneva, for the hydropathy plots and to C. Nager, Biocenter Basel, for comparing the possible ORF 406 translation product with about 2,000 known protein sequences. We thank C. Bachmann for secretarial help and the Fonds National Suisse de la Recherche Scientifique for support (E.S. 183.82). This work is part of the Ph.D thesis of Etienne Roux.

References

Cohen SW, Chang ACY, Hsu L (1972) Proc Natl Acad Sci USA 69:2110–2114
El-Gewely M, Helling RB, Dibbits JGTh (1984) Mol Gen Genet 194:432–443
Flamant F, Heizmann P, Nigon V (1984) Curr Genet 8:9–13
Graf L, Kössel H, Stutz E (1980) Nature 286:908–910
Graf L, Roux E, Stutz E, Kössel H (1982) Nucleic Acids Res 10:6369–6381
Hallick RB (1984) In: Buetow DE (ed) The Biology of Euglena, vol IV. Academic Press, New York, in press
Jenni B, Stutz E (1979) FEBS Lett 102:95–99
Jenni B, Fasnacht M, Stutz E (1981) FEBS Lett 125:175–179
Karabin GD, Narita JO, Dodd JR, Hallick RB (1983) J Biol Chem 258:14790–14796
Koller B, Delius H (1982a) Mol Gen Genet 188:305–308
Koller B, Delius H (1982b) FEBS Lett 140:198–202
Koller B, Delius H, Helling RB (1984) Plant Mol Biol 3:127–136
Kyte J, Doolittle RF (1982) J Mol Biol 157:105–132
Messing J, Vieira J (1982) Gene 19:269–276
Messing J, Crea R, Seeberg Ph (1980) Nucleic Acids Res 9:309–321
Ravel-Chapuis P, Flamant F, Nicolas P, Heizmann P, Nigon V (1984) Nucleic Acids Res 121:1039–1048
Roux E, Graf L, Stutz E (1983) Nucleic Acids Res 11:1957–1968
Sanger F, Coulson AR, Barrel BG, Smith AJH, Roe BA (1980) J Mol Biol 143:161–178
Schlunegger B, Fasnacht M, Stutz E, Koller B, Delius H (1983) Biochim Biophys Acta 739:114–121
Starlinger P (1977) Annu Rev Genet 11:103–126
Starr RC (1964) Am J Bot 51:1013–1044
Tait RC, Rodriguez RL, West RW (1980) J Biol Chem 255:813–815
Wartell RM, Reznikoff WS (1980) Gene 9:307–310

Communicated by U. Leupold

Received October 20, 1984